



Institutionen för vattenbyggnad  
Chalmers Tekniska Högskola  
Department of Hydraulics  
Chalmers University of Technology

# Dynamic Analysis of Mooring Cables

Jan Lindahl  
Anders Sjöberg

Report  
Series A:9  
ISSN 0348-1050

Göteborg 1983

---

Address: Department of Hydraulics  
Chalmers University of Technology  
S-412 96 Göteborg, Sweden  
Telephone: 031/810100



LIST OF CONTENTS	Page
PREFACE	
LIST OF CONTENTS	
ABSTRACT	1
NOTATIONS	2
1. INTRODUCTION	5
2. BASIC EQUATIONS	8
2.1 The equations of motion	8
2.2 The elastic model	8
2.3 Forces acting at the cable	9
2.4 The complete equations of motion	11
3. NUMERICAL SOLUTION	13
3.1 Spatial discretization of the cable	13
3.2 The equilibrium equations	17
3.3 The equations of motion	18
4. UNDAMPED FREE VIBRATIONS OF A CABLE SUPPORTED ON A SPRING	21
5. CALCULATION EXAMPLES	25
5.1 Displacement - excited mooring cable	25
5.2 Comparison with analytical solution	28
5.3 Comparison with tests presented by Johansson [18]	29
6. SUMMARY AND CONCLUSIONS	31
ACKNOWLEDGEMENTS	31
REFERENCES	32
FIGURES	34



## PREFACE

The research work presented in this thesis has been carried out by me at the Department of Hydraulics, Chalmers University of Technology, Göteborg, Sweden.

The study deals with dynamics of mooring cables and is a part of the project "Offshore Structures - Wave Forces and Motions", which is sponsored in part by the National Swedish Board for Technical Development. The project, which is currently ongoing, includes plans for further investigations of the dynamics of mooring cables.

Gothenburg, April 13, 1983.

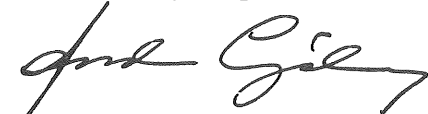


Jan Lindahl

This thesis by Jan Lindahl is to be submitted in partial fulfilment of requirements for the degree of Licentiate of Engineering in Hydraulic Engineering.

I have participated in the preparation of the thesis in my capacity as tutor to Jan Lindahl. It was first presented in the form of a report for the Second International Symposium on Ocean Engineering and Ship Handling, March 1-3, 1983, in Gothenburg, Sweden.

Gothenburg, April 13, 1983



Anders Sjöberg  
Professor



# DYNAMIC ANALYSIS OF MOORING CABLES

J LINDAHL and A SJÖBERG

Chalmers University of Technology, Sweden

## ABSTRACT

A finite element model for numerical analysis of the dynamic response of mooring cables is presented. The model takes into account the elasticity of the cable, inertia forces, drag forces and frictional forces between the sea bottom and the cable. The model is capable of handling both two- and three-dimensional problems. The equations of motion are transformed to ordinary differential equations by means of the virtual work principle. The cable is decomposed into elements connected by nodes. For each node the discretized equations of motion are formulated with the displacement of the node as dependent variable. The equations are then solved by means of a simple explicit time integration method based on a central difference formula. The description of the model is considered complete enough to make an understanding of the construction of the model possible. Calculation examples dealing with a displacement excited mooring cable (chain) are presented where two- and three-dimensional calculations are compared. The calculation results show that the risk of obtaining slack, defined as negative strain, grows with increasing drag force. In a three-dimensional case a relatively long time integration is required to obtain a steady-state.

A comparison is made with an analytical solution in the case of displacement excitations out of the plane of the cable as well as with calculation results presented in the literature.

# NOTATION

Symbol Definition

$\underline{\underline{A}}$	Matrix containing shape functions
$\underline{\underline{\tilde{A}}}$	Matrix containing functions
(A)	Arbitrary time-dependent configuration of the cable (fig. 2.1)
$A_i$	Displacement excitation amplitude
$a$	Constant defined by (4.5)
$\underline{\underline{B}}$	$= \frac{\partial \underline{\underline{A}}}{\partial \underline{\underline{\xi}}_j}$
$C_{DT}$	Tangential drag coefficient
$C_{DN}$	Normal drag coefficient
$C_{MN}$	Hydrodynamic mass coefficient
$C_2$	Constant, defined by (2.16)
$C_3$	Constant, defined by (2.18)
$C_4$	Constant, defined by (2.20)
$\underline{\underline{C}}_j$	Connectivity matrix
$c_c$	Damping constant due to internal friction in the cable
$c_{ij}^{(k)}$	Inverse of the mass matrix of a node (k)
$c_l$	Longitudinal wave velocity
$c_n$	Angles defined by (4.23)
$c_v$	Tolerance in the friction model (fig. 3.2)
$D$	Water depth
$\underline{\underline{D}}_1$	$= \underline{\underline{A}}^t \underline{\underline{B}}$
$\underline{\underline{D}}_2$	$= \underline{\underline{\tilde{A}}}^t \underline{\underline{B}}$
$d_o$	Representative diameter of the cable
$\underline{\underline{E}}_1$	$= \underline{\underline{A}}^t \underline{\underline{A}}$
$\underline{\underline{E}}_2$	$= \underline{\underline{\tilde{A}}}^t \underline{\underline{\tilde{A}}}$
$\underline{\underline{F}}$	Global internal force vector in (A)
$\underline{\underline{F}}_f$	Frictional force acting at the node (k)
$\underline{\underline{F}}_o$	Global internal force vector in (R)
$\underline{\underline{f}}$	$= \underline{\underline{f}}^{(1)} + \underline{\underline{f}}^{(2)} + \underline{\underline{f}}^{(3)}$
$\underline{\underline{f}}^{(1)}$	Hydrostatic and gravitational force vector per unit of unstretched length of the cable in (A) and (R)
$\underline{\underline{f}}^{(2)}$	Tangential drag force vector per unit unstretched length of the cable in (A)
$\underline{\underline{f}}^{(3)}$	Normal drag force vector per unit of unstretched length of the cable in (A)
$\underline{\underline{f}}^{(4)}$	Hydrodynamic inertia force vector per unit of unstretched length of cable in (A)
$\underline{\underline{f}}_r$	Volume and surface forces per unit of unstretched length of cable in (A), the resultant to $\underline{\underline{f}}^{(1)}, \underline{\underline{f}}^{(2)}, \underline{\underline{f}}^{(3)}, \underline{\underline{f}}^{(4)}$
$\underline{\underline{G}}$	$= \underline{\underline{B}}^t \underline{\underline{B}}$
$g$	Gravitational acceleration
$H$	Horizontal component of the cable tension in a static case
$K$	Stiffness of the cable
$K_f$	Spring constant



Symbol	Definition
$L$	Total unstretched length of cable
$l$	The unstretched length of the cable in a simplified model (fig. 4.1)
$l_j$	Unstretched length of the cable element $j$
$l_{jmin}$	Length of the shortest element
$l^*$	Nondimensional length of the cable ( $\approx 1$ for small values of $\theta$ )
$\underline{M}$	Global mass matrix
$\underline{m}_j$	Mass matrix of the element
$N^{(k)}$	Normal force from the bottom acting at a node $(k)$
$ND$	Number of dimensions
$n_e, NE$	Number of elements
$\underline{p}$	Global nodal displacement vector from (R) to (A)
$\underline{p}_i^{(k)}$	Displacement vector of a node $(k)$
$\underline{p}_j$	Element nodal displacement vector from (R) to (A)
$\underline{p}_j^{(k)}$	Resultant to the forces at a node $(k)$ , due to $\underline{f}^{(1)}$ , $\underline{f}^{(2)}$ and $\underline{f}^{(3)}$
$\underline{R}$	Global external load vector due to $\underline{f}^{(1)}$ , $\underline{f}^{(2)}$ and $\underline{f}^{(3)}$
(R)	A configuration of the cable used as a reference configuration, chosen as the static configuration due to gravity and hydrostatic pressure
$\underline{R}$	Global external load vector in (R) due to $\underline{f}^{(1)}$ , $\underline{f}^{(2)}$ and $\underline{f}^{(3)}$
$\underline{R}_j^{(1)}$	Element force vector due to gravity forces and hydrostatic pressure
$\underline{R}_j^{(2)}$	Element force vector due to tangential drag forces
$\underline{R}_j^{(3)}$	Element force vector due to normal drag forces
$\underline{R}_s$	Global force vector in (R) due to the sea bottom, simulated as bilinear springs
$\underline{r}_i^{(k)}$	Position vector of a node $(k)$ in (A)
$\underline{r}_j$	Element nodal position vector in (A)
$\underline{r}_o$	Global nodal position vector in (R)
$\underline{r}_{oj}$	Element nodal position vector in (R)
$s$	Arc length of the stretched cable to a material point P, measured in (A) (fig. 2.1)
$s_j$	Unstretched length of cable measured to "the beginning" of element $j$ (defines the first node of the element for increasing $s_o$ )
$s_o$	Unstretched length of cable measured to a material point P (fig. 2.1)
$T$	Cable tension in (A)
$T_p$	Displacement excitation period
$T_n$	Eigenperiod
$t$	Time
$\Delta t$	Timestep
$\hat{t}$	Unit tangent vector to the cable curve pointing in the direction of increasing arc length measured in (A)
$\underline{u}$	Displacement vector from (R) to (A)

Symbol	Definition
$\underline{v}$	Relative velocity vector of the water (relative to the cable in (A) defined by (2.14))
$\underline{v}_c$	Water velocity vector
$\underline{v}_{cj}$	Water velocity vector for the element in (A)
$\underline{v}_j$	Relative water velocity vector for the element (relative to the element in (A))
$\underline{w}$	Nondimensional displacement vector, $= \underline{u}/l$
$\tilde{w}_{2n}, \tilde{w}_{3n}$	Normal modes
$x$	Nondimensional variable defined by (4.9)
$\underline{x}$	Position vector of the cable in (A) (fig. 2.1)
$\underline{x}_o$	Position vector of the cable in (R) (fig. 2.1)
$\frac{\partial}{\partial s_o}$	
$\frac{\partial}{\partial t}$	
$\vec{\phantom{x}}$	Vector notation
$\mathbf{\phantom{x}}$	Matrix notation
$\alpha$	Strain of the cable at the lowest point for an equilibrium configuration (fig. 4.1)
$\beta$	Parameter representing the influence of the spring
$\bar{\gamma}$	Defined by (4.13c)
$\gamma_o$	Cable mass per unit unstretched length
$\gamma_r$	Reduced mass per unit unstretched length of the cable defined by (2.13)
$\delta \underline{p}$	Global nodal virtual displacement vector
$\epsilon$	Strain of the cable in (A), defined by (2.2)
$\tilde{\epsilon}$	Strain of the cable in (A), defined by (2.4)
$\epsilon_j$	Strain of the element in (A), defined by (3.12a)
$\tilde{\epsilon}_j$	$= \tilde{\epsilon}_{oj} + \Delta \tilde{\epsilon}_j$ . Strain of the element in (A)
$\epsilon_o$	Strain of the cable in (R), defined by (2.11a)
$\tilde{\epsilon}_{oj}$	Strain of the element in (R) defined by (3.12c)
$\Delta \tilde{\epsilon}$	Incremental strain of the cable between the configuration (A) and (R)
$\Delta \tilde{\epsilon}_j$	Incremental strain of the element between configuration (A) and (R)
$\eta$	Parameter representing the stiffness and the geometrical properties of the cable
$\theta$	$= 1/a$ , defining the shallowness of the cable
$\lambda$	Defined by (4.13a)
$\mu$	Bottom friction coefficient
$\xi_j$	Local variable over the element $j$ defined by (3.2). A measure of $s_o$ for the element
$\rho_k$	Density of the cable
$\rho_v$	Density of the water
$\tau$	Characteristic time
$\omega$	Angular frequency

## 1. INTRODUCTION

The purpose of a mooring or a mooring system is to keep the moored vehicle, e.g. a ship, platform or floating factory, in station. A ship may have a one-point mooring while platforms normally use a system of mooring lines. For large structures the mooring lines normally consist of chains or wires. This study has been carried out with mainly these types of lines in mind.

A floating structure is exposed to the influence of wind, currents, and waves. Forces generated by wind and currents are normally assumed to be constant. The forces imposed by the waves may be divided into first-order forces with the same period as the waves, and second order forces, called slow drift forces [1]. The drift force is considered as constant in regular waves and slowly varying in irregular waves. Since the properties of the various forces differ, the moored structure is exposed to drift and oscillatory motions of different time scales.

In calculations of the oscillatory motion of large floating structures, the interaction between the mooring system and the structure is often described by means of simplified models, i.e. without considering the dynamic response of the mooring lines [2]. However, even if simplified models normally seem justified for large structures, the determination of the suitability of certain assumptions has to be based on an analysis of the properties of the moored structure and the environmental conditions, such as resonance periods, wave periods and the mass, damping and stiffness, of the mooring system relative to the corresponding properties of the moored object. In regular waves the oscillatory motion of a ship is very little influenced by the response of a mooring cable if the ship is greater than 1000 tons [3]. In analysis of the motions of, for example, a one-point moored buoy, a dynamic analysis of the complete system is much more important. For further discussion concerning the interaction between the structure and the moorings, reference is made to [4].

In this study the displacement or the force at the upper end of the cable is presumed to be known. We are only interested in the forces and the motions of the cable. The main aspect is thus a detailed dynamic analysis of the mooring cable, only. Such an analysis constitutes an important step towards safer anchorage systems.

Cables may be regarded as long and slender structures and cannot as a rule respond to external loads without a significant change of shape. This property may give major nonlinear effects. The drag forces acting on the cable give rise to important non-linear terms in the governing differential equations. Boundary conditions, as the contact between the cable and the bottom, also constitute essential non-linearities. Therefore in most cases the solution of practical problems, with reference to the dynamic response of cables, requires the use of numerical models implemented on computers. A series of calculation models have been constructed through the years. A brief review with the emphasis on mooring cables is given below. The description makes no claim to

being complete, but it is believed to be important as a background to the model presented in this report.

The most frequently used methods are finite difference methods (FDM), finite element methods (FEM), the "method of characteristics" and perturbation methods.

The starting-point is normally a formulation of the governing partial differential equations or some related variational formulation. Some researchers take a shortcut and divide the cable into segments with certain properties. The equations of motions are then formulated directly as a system of ordinary differential equations.

The partial differential equations may be discretized both in time and space and then numerically solved by means of FDM [5,6]. Maltuk [7] used Hamilton's principle as a variational formulation and applied FDM in both time and space in a study of the stress in a towing wire due to an airplane turn. It is also possible to use the method of characteristics to formulate a number (four in the case of a two-dimensional problem) of ordinary differential equations (the characteristic equations), which may be integrated along their characteristic directions by means of FDM. A mathematical description of the method of characteristics can be obtained in [8] and examples of application to cables in [3,9,10].

Walton and Polachek [11] developed a model where the cable was replaced by a series of masses attached to a weightless inextensible line. The resulting ordinary differential equations were solved by FDM.

Recently, a description of a model [12, 13] has been given, where the cable could be simulated as a series of  $N$  rigid links connected by spherical joints.

Dominques [14] used a model with straight, weightless cable segments (which may be considered as either rigid or elastic) to obtain the small displacement dynamic response of statically deformed cable systems. The solution in the time domain is obtained by a modal analysis technique.

Applications of the finite element method (FEM) to cable problems have been made by [15-20]. FEM is used for discretization in space to obtain time-dependent ordinary differential equations. Leonard and Recker [15] studied the response of sagged cables. The analyses were later extended to cable-nets [16], and curved elements were introduced [17]. An incremental solution technique was used.

Johansson [18] formulated FEM based on linear shape functions for a mooring cable. To obtain a solution in the time domain normal coordinates were introduced in the discretized equations of motion. Because of the non-linear force term a coupling exists between the equations.

The coupled force terms were decoupled by assuming each to be a function of time only, over a short interval of time. A trial and error process was then used to obtain the final state at the end of the interval.

Webster [19] used FEM to calculate the static and dynamic response of general three-dimensional cable structures in a moving fluid. He also used different techniques to solve the resulting non-linear algebraic equations or non-linear ordinary differential equations.

In an attempt to minimize the computing time [20], a number of numerical techniques were compared to determine the dynamic response of a net of electrical high-tension cables. Higher order shape functions were used, both explicit and implicit time integration procedures were tested.

The perturbation method is used in [21,22]. Goodman and Breslin [21] outlined a method for the solution of the linearized cable-buoy dynamic equations. Triantafyllou [22] presents a perturbation method based on multiple-time-scale expansion for the preliminary design of mooring systems.

Several of the above-mentioned studies deal with the dynamics of underwater cables from various aspects [3,9,11,12,13,14,18,19,21,22]. A cable can be represented by different types of physical models. In the studies cited, the formulation varies from elasto-plastic models dealing with large strains to axial-stiff models and from models assuming small oscillation to models accepting large ones. We are of the opinion that dynamic analyses of mooring cables require consideration of the elasticity of the cable also in case of small strains. The elastic model used in this study is consistent with the one in [20], if the strains are small.

The perturbation method offers valuable possibilities of accomplishing rapid results by means of solutions in the frequency domain or by parametric analysis. In order to obtain a direct numerical solution of the governing non-linear differential equations with respect to, for example, non-linear drag forces (which may be of significant magnitude) methods like FDM, FEM, and the method of characteristic can be used. When these methods are used, there is a great need of checking whether the numerical solution is consistent with the solution of the corresponding differential equations. This is not an easy task due to the non-linearity of the problem. However, verification of numerical models requires comparison with known analytical solutions. Comparisons with solutions obtained by other existing numerical models may strengthen the confidence in a model. In this study only results from preliminary comparisons are presented.

In the numerical model presented in this paper, the governing differential equations have been formulated with the displacements as dependent variables. The finite element model is used for the discretization of the equations into a system of time-dependent ordinary differential equations. The time integration of the equations is carried out by means of a simple explicit numerical method, which results in easy programming without iterations or solutions of systems of equations. It also makes it easy to test different formulations of the model and to make additions to the model.

This study is part of the work for a thesis performed by the first author.

## 2. BASIC EQUATIONS

### 2.1 The equations of motion

A mooring cable is regarded as a long slender structure with negligible moments and shear forces. The only internal force considered is the tension  $T$ , tangential to the local cable direction.

The equations of motion of a cable in rectangular Cartesian coordinates are well known [23,24]. They may be written with the unstretched length  $s_0$ , measured along the cable from the end point ( $s_0 = 0$ ) to a material point  $P$ , as an independent variable (Fig. 2.1). Let  $ds$  be a small element of the cable measured in an arbitrary time dependent configuration (A). Assuming the mass of this element to be constant, we obtain using vector notations,

$$\gamma_0 \ddot{\underline{x}} - \frac{\partial}{\partial s_0} (T \hat{t}) - \underline{f}_r = \underline{0} \quad (2.1)$$

where  $\gamma_0$  is the cable mass per unit of unstretched length,  $T$  is the cable tension,  $\hat{t}$  is the unit tangent vector to the cable curve,  $\underline{x}$  is the position vector of the point  $P$  and  $\underline{f}_r$  represents volume forces and surface forces per unit of unstretched length of the cable. The symbols,  $\cdot$ , and  $\ddot{\cdot}$ , refer to  $\partial/\partial t$  and  $\partial^2/\partial t^2$ , respectively.

The variables  $T$ ,  $\hat{t}$ ,  $\underline{f}_r$  and  $\underline{x}$  are functions of the independent variables  $s_0$  and time  $t$  within the intervals  $s_0 \in [0, L]$  and  $t \in [0, \tau]$ , respectively.  $L$  is the total unstretched length of the cable.  $\tau$  is some characteristic time.

The arc length of the stretched configuration to the point  $P$  is denoted  $s$ .

### 2.2 The elastic model

For a short element  $ds_0$ , strain is defined by the equation

$$\epsilon = s' - 1 \quad (2.2)$$

where  $s' = \partial/\partial s_0$ . The unit tangent vector may then be written

$$\hat{t} = \frac{\underline{x}'}{1 + \epsilon} \quad (2.3)$$

We also introduce the strain

$$\tilde{\epsilon} = \frac{1}{2}(s'^2 - 1) = \frac{1}{2}(\underline{x}' \cdot \underline{x}' - 1) \quad (2.4)$$

which is related to  $\epsilon$  by the equation

$$(1 + \epsilon)^2 = 1 + 2\tilde{\epsilon} \quad (2.5)$$

Let us now assume the cable to follow the constitutive relation

$$T = K\tilde{\epsilon}(1 + \epsilon) \quad (2.6)$$

where  $K$  is a constant dependent on the elasticity of the cable. Restricting the analysis to small strains,  $0 < \epsilon \ll 1$ , we find that

$$T = K\tilde{\epsilon}(1+\epsilon) \approx K\tilde{\epsilon} \approx K\epsilon \quad (2.7)$$

i.e., equation (2.6) follows Hooke's law,  $T = K\epsilon$ . The reason for introducing Eq.(2.6) as a constitutive law is to avoid complications in later stages of the analysis.

Substituting Eqs.(2.3) and (2.6) into Eq.(2.1) now gives

$$\gamma_0 \ddot{\underline{x}} - \frac{\partial}{\partial s_0} (K\tilde{\epsilon} \underline{x}') - \underline{f}_r = \underline{0} \quad (2.8)$$

It has been judged advantageous to relate the displacements of the cable to some known cable configuration. A reference configuration (R) is thus defined by the position vector  $\underline{x}_0(s_0)$ , (Fig. 2.1), and the strain  $\tilde{\epsilon}_0(s_0)$ . If  $\underline{u}$  is the displacement and  $\Delta\tilde{\epsilon}$  is the incremental strain between the actual configuration (A) and the reference configuration (R),

$$\begin{aligned} \underline{x} &= \underline{x}_0 + \underline{u} \\ \tilde{\epsilon} &= \tilde{\epsilon}_0 + \Delta\tilde{\epsilon} \end{aligned} \quad (2.9)$$

which substituted into Eqs.(2.8) and using (2.4) gives

$$\gamma_0 \ddot{\underline{u}} - \frac{\partial}{\partial s_0} (K(\tilde{\epsilon}_0 + \Delta\tilde{\epsilon})(\underline{x}_0' + \underline{u}')) - \underline{f}_r = \underline{0} \quad (2.10)$$

where

$$\tilde{\epsilon}_0 = \frac{1}{2} (\underline{x}_0' \cdot \underline{x}_0' - 1) \quad (2.11a)$$

$$\Delta\tilde{\epsilon} = \frac{1}{2} (\underline{u}' \cdot \underline{u}' + \underline{x}_0' \cdot \underline{u}') \quad (2.11b)$$

The equations of motion as given by Eq.(2.10) seem to be consistent with the ones given in [20] apart from the choice of reference configuration, which in [20] is chosen as  $\tilde{\epsilon}_0 = 0$ . (They also included temperature effects and electro dynamic forces).

The reason for the derivation of the equations in this section is that we wanted to explain the expression (2.7).

### 2.3 Forces acting at the cable

The force  $\underline{f}_r$  acting at the cable is composed of gravity forces, hydrostatic forces, and hydrodynamic forces.

This study is limited to cables in stationary water currents. The water velocity  $\underline{v}_c$  is assumed to be parallel to the water surface and slowly varying from the bottom to the surface. The hydrodynamic forces are caused by the relative velocity between the water and the cable and by the acceleration of

the cable. A summary of different approaches is given in [25].

The Cartesian coordinates  $x_1$  and  $x_3$  lie in the plane of the sea bottom parallel to the water surface (Fig. 2.1).  $x_2$  is vertical and positive upwards. At the bottom  $x_2 = 0$ . The water surface is defined by  $x_2 = D$ , where  $D$  is the water depth.

#### Hydrostatic force and gravity force

The hydrostatic force at a cable element  $ds$  is caused by the hydrostatic pressure on the surface of the element. For a chain the pressure may be assumed to be distributed all over the surface, including the end faces of the element, each link being totally surrounded by water.

In the case of a wire this assumption is less exact. A more exact procedure requires here subtraction of the pressure integral over the end faces of the element [18,21]. However, the assumption of an element completely surrounded by water seems justified also for wires. It is believed that the errors induced by this assumption are negligible in this application.

Each element,  $ds$ , is thus regarded as completely surrounded by water. It is also assumed that the volume of the element remains constant. The resultant  $\underline{f}^{(1)}$  to the hydrostatic pressure and the gravity forces is then obtained as the weight of the cable per unit of unstretched length minus the weight of the displaced water,

$$\underline{f}^{(1)} = [0, -\gamma_r g, 0]^T \quad (2.12)$$

where

$$\gamma_r = \frac{\rho_k - \rho_v}{\rho_k} \gamma_o \quad (2.13)$$

and  $\rho_k$  is the cable mass density and  $\rho_v$  the water mass density.

#### Hydrodynamic forces

The physical modelling of the hydrodynamic forces is based on the Morison equation. The model is of the same type as those presented in [18,19]. Johansson [18] also includes the effect of an accelerating flow field. Webster [19] uses variable drag coefficients depending on the actual flow condition. The vector formulation of the forces may be obtained from [18].

The hydrodynamic forces are formulated for a cable of circular cross-section with a "drag diameter"  $d_o$ , constant within each element  $ds$ . In the case of a chain,  $d_o$  is some characteristic length.

The relative velocity between the water and the cable is

$$\underline{v} = \underline{v}_c - \dot{\underline{u}} \quad (2.14)$$



The tangential component  $\underline{v} \cdot \hat{t}$  gives a drag force,  $\underline{f}^{(2)}$ , per unit of unstretched length, expressed as

$$\underline{f}^{(2)} = C_2 |\underline{v} \cdot \hat{t}| \underline{v} \cdot \hat{t} (1+\epsilon) \quad (2.15)$$

where

$$C_2 = \frac{1}{2} C_{DT} d_o \rho_v \quad (2.16)$$

$C_{DT}$  is a tangential drag coefficient.

In the direction normal to the cable, the relative velocity gives the drag force  $\underline{f}^{(3)}$  per unit of unstretched length,

$$\underline{f}^{(3)} = C_3 |\underline{v} - \underline{v} \cdot \hat{t} \hat{t}| (\underline{v} - \underline{v} \cdot \hat{t} \hat{t}) (1+\epsilon) \quad (2.17)$$

where

$$C_3 = \frac{1}{2} C_{DN} d_o \rho_v \quad (2.18)$$

$C_{DN}$  is a drag coefficient in the direction normal to the cable.

Finally, the acceleration of the cable in the normal direction is assumed to give rise to the hydrodynamic inertia force  $\underline{f}^{(4)}$  per unit of unstretched length,

$$\underline{f}^{(4)} = -C_4 (\ddot{\underline{u}} - \ddot{\underline{u}} \cdot \hat{t} \hat{t}) (1+\epsilon) \quad (2.19)$$

where

$$C_4 = C_{MN} \frac{\pi d_o^2}{4} \rho_v \quad (2.20)$$

$C_{MN}$  is a hydrodynamic mass coefficient. The coefficients  $C_{DT}$ ,  $C_{DN}$  and  $C_{MN}$  are all considered constant.

The inertia force in the tangential direction of the cable has here been neglected, even though it should not lead to any major difficulties in the formulation of the equations. If this force is considered important, the constant  $C_4$  in the third term of Eq. (2.21) below may be exchanged for another constant.

#### 2.4 The complete equations of motion

The force  $\underline{f}_r$  in Eq. (2.10) is thus the resultant of the forces  $\underline{f}^{(1)}$ ,  $\underline{f}^{(2)}$ ,  $\underline{f}^{(3)}$  and  $\underline{f}^{(4)}$ . Substitution of the corresponding equations and using (2.3) gives after some algebra

$$\gamma_o \ddot{\underline{u}} + C_4 (1+\epsilon) \ddot{\underline{u}} - \frac{C_4}{1+\epsilon} (\ddot{\underline{u}} \cdot \underline{x}) \underline{x} - \frac{\partial}{\partial s_o} (K \hat{E} \underline{x}) - \underline{f} = \underline{0} \quad (2.21)$$

where

$$\underline{f} = \underline{f}^{(1)} + \underline{f}^{(2)} + \underline{f}^{(3)} \quad (2.22)$$

$$\underline{f}^{(1)} = [0, -\gamma_{\underline{x}} g, 0]^T \quad (2.23)$$

$$\underline{f}^{(2)} = c_2 |\underline{v} \cdot \underline{x}^-| (\underline{v} \cdot \underline{x}^-) \underline{x}^- \frac{1}{(1+\epsilon)^2} \quad (2.24)$$

$$\underline{f}^{(3)} = c_3 (\underline{v} \cdot \underline{v} - \frac{1}{(1+\epsilon)^2} (\underline{v} \cdot \underline{x}^-)^2)^{1/2} (\underline{v} - (\underline{v} \cdot \underline{x}^-) \underline{x}^- \frac{1}{(1+\epsilon)^2}) (1+\epsilon) \quad (2.25)$$

$$\underline{x}^- = \underline{x}_O^- + \underline{u}^- \quad (2.26)$$

$$\underline{v} = \underline{v}_C - \dot{\underline{u}} \quad (2.27)$$

$$(1+\epsilon)^2 = 1+2\tilde{\epsilon} \quad (2.28)$$

$$\tilde{\epsilon} = \tilde{\epsilon}_O + \Delta\tilde{\epsilon} \quad (2.29)$$

$$\tilde{\epsilon}_O = \frac{1}{2} (\underline{x}_O^- \cdot \underline{x}_O^- - 1) \quad (2.30)$$

$$\Delta\tilde{\epsilon} = \frac{1}{2} \underline{u}^- \cdot \underline{u}^- + \underline{x}_O^- \cdot \underline{u}^- \quad (2.31)$$

### 3. NUMERICAL SOLUTION

#### 3.1 Spatial discretization of the cable

The equations of motion (2.21) are a set of nonlinear partial differential equations. These equations may be transformed to ordinary differential equations by means of the virtual work principle. The use of this principle in finite element analysis is described in [26].

Let the cable be subject to a small displacement  $\delta \underline{u}$  in relation to the configuration (A) at time  $t$ . The virtual work done by the forces is then:

$$\int_0^L \{ (\gamma_0 \ddot{\underline{u}} + C_4(1+\epsilon) \ddot{\underline{u}} - \frac{C_4}{1+\epsilon} (\ddot{\underline{u}} \cdot \underline{x}') \underline{x}') \cdot \delta \underline{u} - \underline{f} \cdot \delta \underline{u} + K \ddot{\underline{x}}' \cdot \delta \underline{u}' \} ds_0 - [K \ddot{\underline{x}}' \cdot \delta \underline{u}]_0^L = 0 \quad (3.1)$$

Eq. (3.1) is obtained by taking the scalar product of Eq. (2.21) and  $\delta \underline{u}$  and integrating over the unstretched length  $L$  of the cable. The last term is obtained by partial integration. It represents the virtual work performed by forces acting at the end faces of the cable.

The cable is now decomposed into a number of  $n_e$  disjointed elements, called finite elements, with the unstretched length  $l_j$ . Over the element  $j$ , the unstretched length  $s_0$  is expressed by

$$\begin{aligned} s_0 &\in [0, L] \\ s_0 &= s_j + \xi_j l_j \quad \xi_j \in [0, 1] \\ n_e \\ L &= \sum_{j=1} l_j \end{aligned} \quad (3.2)$$

where  $s_j$  defines "the beginning" of the element. By means of Eq. (3.2) the variable  $s_0$  is exchanged for  $\xi_j$ , for example  $\underline{u} = \underline{u}(\xi_j, t)$  for each element  $j$ .

For the sake of simplicity we for the moment assume the last term in Eq. (3.1) to be zero. This would be the case if the cable was completely free or if displacements are prescribed for  $s_0=0$  and  $s_0=L$ . As the elements are disjointed, we may rewrite Eq. (3.1) using Eq. (3.2)

$$\begin{aligned} \sum_{j=1}^{n_e} \int_0^1 \{ (\gamma_0 \ddot{\underline{u}} + C_4(1+\epsilon) \ddot{\underline{u}} - \frac{C_4}{(1+\epsilon)l_j^2} (\ddot{\underline{u}} \cdot \frac{\partial \underline{x}}{\partial \xi_j}) \frac{\partial \underline{x}}{\partial \xi_j}) \cdot \delta \underline{u} - \underline{f} \cdot \delta \underline{u} + \frac{K \ddot{\underline{x}}}{l_j^2} \frac{\partial \underline{x}}{\partial \xi_j} \cdot \frac{\partial}{\partial \xi_j} (\delta \underline{u}) \} l_j d\xi_j &= 0 \end{aligned} \quad (3.3)$$

Over each finite element  $j$ , all variables are assumed to be continuous and approximated by the following relations

$$\begin{aligned}
\underline{u}(\xi_j, t) &= \underline{A}(\xi_j) \underline{p}_j(t) \\
\underline{x}_o(\xi_j) &= \underline{A}(\xi_j) \underline{r}_{oj} & \xi_j \in [0,1] \\
\underline{x}(\xi_j, t) &= \underline{A}(\xi_j) \underline{r}_j(t) & j = 1, n_e \\
\underline{v}(\xi_j, t) &= \underline{A}(\xi_j) \underline{v}_j(t) \\
\underline{v}_c(\xi_j, t) &= \underline{A}(\xi_j) \underline{v}_{cj}(t) \\
\delta \underline{u}(\xi_j, t) &= \underline{A}(\xi_j) \delta \underline{p}_j(t)
\end{aligned} \tag{3.4a,b,c,d,e,f}$$

where the matrix  $\underline{A}$  contains the so-called shape functions, which are here assumed to be linear,

$$\underline{A} = \begin{bmatrix} 1-\xi_j & 0 & 0 & \xi_j & 0 & 0 \\ 0 & 1-\xi_j & 0 & 0 & \xi_j & 0 \\ 0 & 0 & 1-\xi_j & 0 & 0 & \xi_j \end{bmatrix} \tag{3.5}$$

and where

- $\underline{p}_j$  = element nodal displacement vector
- $\underline{r}_{oj}$  = element nodal position vector in configuration (R)
- $\underline{r}_j$  = element nodal position vector in configuration (A)
- $\underline{v}_j$  = element nodal relative velocity vector
- $\underline{v}_{cj}$  = element water velocity vector
- $\delta \underline{p}_j(t)$  = element nodal virtual displacement vector

It follows directly from Eqs. (2.9), (2.14) and (3.4) that

$$\begin{aligned}
\underline{r}_j &= \underline{r}_{oj} + \underline{p}_j \\
\underline{v}_j &= \underline{v}_{cj} - \dot{\underline{p}}_j
\end{aligned} \tag{3.6a,b}$$

All the vectors given above have the dimension  $(6 \times 1)$ . The elements have two nodes, each with three degrees of freedom. The first three components describe the conditions at one node ( $s_o = s_j$ ) and the last three at the other node ( $s_o = s_j + 1_j$ ).

In order to obtain an easily invertible mass matrix, we make the following approximation with respect to accelerations and virtual displacements associated with the inertia forces:

$$\begin{aligned}
\ddot{\underline{u}}(\xi_j, t) &= \tilde{\underline{A}} \ddot{\underline{p}}_j(t) & \xi_j \in [0,1] \\
\delta \underline{u}(\xi_j, t) &= \tilde{\underline{A}} \delta \underline{p}_j(t) & j = 1, n_e
\end{aligned} \tag{3.7}$$

The matrix  $\tilde{\underline{A}}$  is chosen

$$\underline{\tilde{A}} = \begin{bmatrix} \varphi_1 & 0 & 0 & \varphi_2 & 0 & 0 \\ 0 & \varphi_1 & 0 & 0 & \varphi_2 & 0 \\ 0 & 0 & \varphi_1 & 0 & 0 & \varphi_2 \end{bmatrix} \quad (3.8)$$

where

$$\varphi_1 = 1 \quad \text{and} \quad \varphi_2 = 0 \quad \text{for} \quad \xi_j \in [0, 1/2]$$

$$\varphi_1 = 0 \quad \text{and} \quad \varphi_2 = 1 \quad \text{for} \quad \xi_j \in [1/2, 1]$$

The nodal vectors of element  $j$  are related to the corresponding global vectors through the connectivity matrix  $\underline{C}_j$ , for example

$$\begin{aligned} \underline{p}_j &= \underline{C}_j \underline{p} \\ \underline{r}_{oj} &= \underline{C}_j \underline{r}_o \quad j=1, n_e \\ \delta \underline{p}_j &= \underline{C}_j \delta \underline{p} \end{aligned} \quad (3.9)$$

where  $\underline{p}$  = global nodal displacement vector,

$\underline{r}_o$  = global nodal coordinate vector in configuration (R), and  $\delta \underline{p}$  = global nodal virtual displacement vector.

The global vectors and the connectivity matrix  $\underline{C}_j$  have the dimensions  $(n \times 1)$  and  $(6 \times n)$ , respectively, where  $n$  is the number of degrees of freedom of the total system.

Substituting Eqs. (3.4), (3.7) and (3.9) into Eq. (3.3) gives

$$\begin{aligned} \sum_{j=1}^{n_e} \int_0^1 \delta \underline{p}^T \{ [\underline{C}_j^T \underline{l}_j (\gamma_o + C_4 (1 + \epsilon_j)) \underline{E}_2 \underline{C}_j \ddot{\underline{p}} - \underline{C}_j^T \frac{C_4}{(1 + \epsilon_j) \underline{l}_j} \underline{D}_2 \underline{r}_j \underline{r}_j^T \underline{D}_2^T \underline{C}_j \ddot{\underline{p}}] \\ - \underline{C}_j^T \underline{l}_j \underline{A}^T \underline{f} + \underline{C}_j^T \underline{G} \underline{r}_j \frac{K \tilde{\epsilon}_j}{\underline{l}_j} \} d\xi_j = 0 \end{aligned} \quad (3.10)$$

where

$$\begin{aligned} \underline{B} &= \frac{\partial \underline{A}}{\partial \xi_j} \\ \underline{G} &= \underline{B}^T \underline{B} \\ \underline{E}_2 &= \tilde{\underline{A}}^T \tilde{\underline{A}} \\ \underline{D}_2 &= \tilde{\underline{A}}^T \underline{B} \end{aligned} \quad (3.11a,b,c,d)$$

The symbol  $\underline{B}^T$  means the transpose of  $\underline{B}$ .

The strain of element  $j$  follows from Eqs. (2.28)-(2.31), (3.4) and (3.11b),

$$\begin{aligned} (1 + \epsilon_j)^2 &= 1 + 2\tilde{\epsilon}_j \\ \tilde{\epsilon}_j &= \tilde{\epsilon}_{oj} + \Delta \tilde{\epsilon}_j \end{aligned} \quad (3.12a,b)$$

$$\tilde{\epsilon}_{oj} = \frac{1}{2} \left( \frac{1}{l_j^2} \mathbf{r}_{oj}^T \mathbf{G} \mathbf{r}_{oj} - 1 \right) \quad (3.12c,d)$$

$$\Delta \tilde{\epsilon}_j = \frac{1}{2l_j^2} \mathbf{p}_j^T \mathbf{G} \mathbf{p}_j + \frac{1}{2} \mathbf{r}_{oj}^T \mathbf{G} \mathbf{p}_j;$$

Since  $\delta \mathbf{p}$  may be arbitrary in Eq. (3.10), we obtain the equations of motion in the following form:

$$\underline{\underline{M}} \ddot{\underline{\underline{p}}} = \underline{\underline{R}} - \underline{\underline{F}} \quad (3.13)$$

where  $\underline{\underline{M}}$  is the mass matrix of the system,

$$\underline{\underline{M}} = \sum_{j=1}^{n_e} \mathbf{C}_j^T \underline{\underline{m}}_j \mathbf{C}_j \quad (3.14)$$

and  $\underline{\underline{m}}_j$  is the mass matrix of element  $j$ ,

$$\underline{\underline{m}}_j = \int_0^1 \{ l_j (\gamma_o + C_4 (1 + \epsilon_j)) \underline{\underline{E}}_2 - \frac{C_4}{(1 + \epsilon_j) l_j} \underline{\underline{D}}_2 \mathbf{r}_j \mathbf{r}_j^T \underline{\underline{D}}_2^T \} d\xi_j \quad (3.15)$$

The external force vector  $\underline{\underline{R}}$  is defined by the second term in Eq. (3.10). With  $\underline{\underline{f}}$  according to Eq. (2.22), we obtain

$$\underline{\underline{R}} = \sum_{j=1}^{n_e} \mathbf{C}_j^T (\underline{\underline{R}}_j^{(1)} + \underline{\underline{R}}_j^{(2)} + \underline{\underline{R}}_j^{(3)}) \quad (3.16)$$

where  $\underline{\underline{R}}_j^{(1)}$  arises from hydrostatic and gravity forces, Eq. (2.23),

$$\underline{\underline{R}}_j^{(1)} = \int_0^1 l_j \mathbf{A}^T \underline{\underline{f}}^{(1)} d\xi_j \quad (3.17)$$

and  $\underline{\underline{R}}_j^{(2)}$  comes from the tangential drag forces, Eq. (2.24),

$$\underline{\underline{R}}_j^{(2)} = C_2 \int_0^1 \frac{1}{(1 + \epsilon_j)^2 l_j^2} | \underline{\underline{v}}_{j=1}^T \mathbf{r}_j | (\underline{\underline{v}}_{j=1}^T \mathbf{r}_j) \underline{\underline{D}}_1 \mathbf{r}_j d\xi_j \quad (3.18)$$

with  $\underline{\underline{D}}_1 = \mathbf{A}^T \underline{\underline{B}}$ .  $\underline{\underline{R}}_j^{(3)}$  is derived from the drag forces normal to the cable, Eq. (2.25),

$$\underline{\underline{R}}_j^{(3)} = C_3 \int_0^1 l_j (1 + \epsilon_j) \{ \underline{\underline{v}}_{j=1}^T \underline{\underline{v}}_j - \frac{1}{(1 + \epsilon_j)^2 l_j^2} (\underline{\underline{v}}_{j=1}^T \mathbf{r}_j)^2 \}^{1/2} \{ \underline{\underline{E}}_1 \underline{\underline{v}}_j - \frac{1}{(1 + \epsilon_j)^2 l_j^2} (\underline{\underline{v}}_{j=1}^T \mathbf{r}_j) \underline{\underline{D}}_1 \mathbf{r}_j \} d\xi_j \quad (3.19)$$

with  $\underline{\underline{E}}_1 = \mathbf{A}^T \underline{\underline{A}}$ .

The last term in Eq. (3.10) represents the reaction forces  $\underline{\underline{F}}$  of the cable

$$\underline{\underline{F}} = \sum_{j=1}^{n_e} \mathbf{C}_j^T \int_0^1 \frac{K \tilde{\epsilon}_j}{l_j} \underline{\underline{G}} \mathbf{r}_j d\xi_j \quad (3.20)$$

When the matrix  $\underline{\underline{A}}$  is chosen according to Eq. (3.5), numerical integration is required only of Eqs. (3.18) and (3.19). It also follows from Eqs. (3.11) and (3.12) that the strain  $\tilde{\epsilon}_j$  is constant along each element  $j$ . The equations, which may look complicated, are further developed before computer implementation.

The definition of  $\tilde{\underline{A}}$  by Eq. (3.8) gives a simple mass matrix  $\underline{m}_j$ . It has the dimension (6 x 6), and it becomes block diagonal with two matrices (3 x 3) in the diagonal. The rest of the elements in  $\underline{m}_j$  are zero.

### 3.2 The equilibrium equations

The reference configuration (R) is defined by the global nodal coordinate vector  $\underline{r}_0$ , which is derived from the equilibrium equations. In the case of no contact with the sea bottom:

$$\underline{R}^{(1)} - \underline{F}_0 = \underline{0} \quad (3.21)$$

which are obtained from Eq. (3.13) with  $\underline{p}=\underline{0}$  and  $\underline{v}_c=\underline{0}$ , that is for static conditions.  $\underline{R}^{(1)}$  arises from hydrostatic and gravity forces, Eq. (3.17), and  $\underline{F}_0$  is given by

$$\underline{F}_0 = \sum_{j=1}^{n_e} \underline{C}_j^T \int_0^1 \frac{K \tilde{\epsilon}_{oj}}{1_j} \underline{G} \underline{r}_{oj} d\xi_j \quad (3.22)$$

If the positions of the ends of the cable ( $s_0=0; L$ ) are prescribed, the corresponding components are excluded from Eq. (3.21). If instead the supporting forces are given, these are added to the corresponding components of, for example,  $\underline{R}^{(1)}$ .

In the equilibrium case the sea bottom is considered to be smooth and elastic. Bilinear elastic springs are introduced at the nodes of the cable. A spring becomes active only if the node is underneath the bottom. The spring stiffness is chosen to be proportional to the cable stiffness.

The spring force contributions are assembled in the vector  $\underline{R}_s$ . The equilibrium equations then become

$$\tilde{\underline{R}}^{(1)} - \tilde{\underline{F}}_0 + \underline{R}_s = \underline{0} \quad (3.23)$$

The tilde indicates that appropriate boundary conditions have been introduced.

Eq. (3.23) represents a set of non-linear algebraic equations. The equations are solved with respect to  $\underline{r}_0$  by means of successively updated reference configurations (not described here) corresponding to a gradually increased level of strength of gravity forces and hydrostatic forces. When these forces have reached their full strength, the static configuration  $\underline{r}_0$  has been achieved.

The calculations are carried out in two dimensions only, since the cable configuration is in the vertical plane. The component of  $\underline{r}_0$  representing the third dimension is thus put equal to zero. The numerical solution of Eq. (3.23) is carried out by means of a quasi Newton method using an algorithm presented in [27].

The equilibrium configuration constitutes the initial-conditions of the time-dependent analysis.

### 3.3 The equations of motion

We assume that the reference configuration  $\underline{r}_0$  of the cable and the corresponding strains  $\tilde{\epsilon}_{0j}$  have been calculated with Eq. (3.23). For the sake of simplicity we also assume prescribed displacements at the boundaries  $s_0=0,L$  of the cable. The corresponding components of the equations of motion are then excluded (reduced vectors and matrices are denoted  $\tilde{\phantom{x}}$ ). Premultiplying Eq. (3.13) by the inverse  $\underline{\tilde{M}}^{-1}$  of  $\underline{\tilde{M}}$ , we obtain

$$\ddot{\underline{\tilde{p}}} = \underline{\tilde{M}}^{-1} \underline{\tilde{p}} \quad (3.24)$$

where  $\underline{\tilde{p}} = \underline{\tilde{R}} - \underline{\tilde{F}}$ . The mass matrix  $\underline{\tilde{M}}$  is a function of the displacements, while  $\underline{\tilde{p}}$  is a function of both velocities and displacements.

The Eq. (3.24) may be considered as the equations of motion of a discrete system (Fig. 3.1). This fact is made use of when simulating the contact between the cable and the bottom. The equations were established for a freely movable cable, and they have to be modified with regard to the possible contact between the cable and the bottom.

In the time-dependent analysis the sea-bottom is simulated as stiff and energy absorbing. When a node on the cable hits the bottom, it is assumed that all kinetic energy associated with the vertical velocity of the node is absorbed. After the impact the node moves along the bottom affected by frictional forces, until its vertical acceleration becomes greater than zero. Then the node is presumed to be freely movable again.

The components of Eq. (3.24) associated with node (k) may be written

$$\ddot{p}_i^{(k)} = c_{ij}^{(k)} p_j^{(k)} \quad \begin{matrix} i = 1,2,3 \\ j = 1,2,3 \end{matrix} \quad (3.25)$$

where

$$\begin{aligned} p_i^{(k)} &= \text{displacements of node (k)} & i=1,2,3 \\ c_{ij}^{(k)} &= \text{inverse of the mass matrix of the node (symmetric 3 x 3)} \\ p_j^{(k)} &= \text{forces acting at the node (k)} & j=1,2,3 \end{aligned}$$

The equation above holds for all nodes (k) situated above the sea bottom, i.e. if  $r_2^{(k)} > 0$ , where  $r_2^{(k)}$  is the vertical components of the coordinate vector  $\underline{r}_i^{(k)}$ . (In the calculations the bottom is defined within a tolerance level).

When  $r_2^{(k)} \approx 0$ , contact is obtained between the node and the bottom, and the node moves in the plane of the bottom only. The mass matrix is assumed to be unchanged while the equations of motion are modified:

$$\begin{bmatrix} \ddot{p}_1^{(k)} \\ 0 \\ \ddot{p}_3^{(k)} \end{bmatrix} = \begin{bmatrix} c_{11} & c_{12} & c_{13} \\ c_{12} & c_{22} & c_{23} \\ c_{13} & c_{23} & c_{33} \end{bmatrix}^{(k)} \begin{bmatrix} p_1^{(k)} \\ p_2^{*(k)} \\ p_3^{*(k)} \end{bmatrix} \quad (3.26)$$

with



$$\dot{p}_2^{(k)} = 0$$

$$p_2^{*(k)} = p_2^{(k)} + N^{(k)}$$

$$N^{(k)} = \text{normal force from the bottom acting at the node } (k).$$

To the third component of the force vector has been added a frictional force

$$p_3^{*(k)} = p_3^{(k)} + F_f \quad (3.27)$$

The formulation of the frictional force  $F_f$  appears from (Fig. 3.2).

From Eq. (3.26) follows that

$$p_2^{*(k)} = -\frac{1}{c_{22}}(c_{12}p_1^{(k)} + c_{23}p_3^{*(k)}) \quad (3.28)$$

which becomes equal to zero if both of the elements adjoining the node lie on the bottom. Then, the normal force equals the resultant to buoyancy forces and gravity forces acting at the node. Eqs. (3.26)-(3.28) are valid until  $\ddot{p}_2^{(k)} > 0$  according to Eq. (3.25), which means that a force again may lift the node from the bottom.

By using the three-dimensional form of the inverse of the mass matrix in Eq. (3.26), we can use the same formulation whether the node is in contact with the bottom or not. The equations of motion are always formally written on the form

$$\ddot{\tilde{p}} = f(\tilde{p}, \dot{\tilde{p}}) \quad (3.29)$$

The equations are solved by means of an explicit time integration method.

Assume that  $\tilde{p}$  at time  $t$  and  $\dot{\tilde{p}}$  at time  $t$  and  $t-\Delta t/2$  are known. The accelerations at time  $t$  can then be calculated from Eq. (3.29),

$$\ddot{\tilde{p}}^t = f(\tilde{p}^t, \dot{\tilde{p}}^t) \quad (3.30)$$

Then, by means of a central difference formula, we calculate

$$\tilde{p}^{t+\Delta t/2} = \tilde{p}^{t-\Delta t/2} + \Delta t \dot{\tilde{p}}^t \quad (3.31)$$

and by extrapolation, we find

$$\tilde{p}^{t+\Delta t} = \tilde{p}^{t+\Delta t/2} + \frac{1}{2}(\tilde{p}^{t+\Delta t/2} - \tilde{p}^{t-\Delta t/2}) \quad (3.32)$$

Finally, the displacements are found by the central difference formula

$$\tilde{p}^{t+\Delta t} = \tilde{p}^t + \Delta t \dot{\tilde{p}}^{t+\Delta t/2} \quad (3.33)$$

The central difference formula as used in Eqs. (3.31) and (3.33) seems favourable from the point of view of stability of heavily damped systems. The fundamental limit on the time step  $\Delta t$  in this application is (for very high values of  $C_{DN}$  and  $C_{DT}$ , however, still smaller values of  $\Delta t$  have to be used),

$$\Delta t < l_{j \min} / c_1 \quad (3.34)$$

where

$$l_{j \min} = \text{length of the shortest element}$$

$$c_1 = \sqrt{K/\gamma_0} = \text{longitudinal wave velocity in the cable}$$

Eqs. (3.31)-(3.33) have been used earlier for cables in connection with towing

by airplane [7].

An explicit integration method may seem inefficient compared to an implicit solution of Eq. (3.29) considering the small time step required by the explicit method. However, the calculation effort per time step is much less for this method. It leads to simpler and smaller program packages and less complicated programming, which makes testing of different calculation models easier.

The greatest part of the calculation effort is in our case associated with the setting up of the mass matrix, Eq. (3.15) and its inverse and with the calculation of the drag forces, Eqs. (3.18) and (3.19). However, in many cases it might not be necessary to update these at each time step.

For a heavy cable the mass of the cable always dominates in the mass matrix. In the case of small rotations and strains, it should then be possible to use the mass matrix calculated for the equilibrium configuration, that is, to exchange  $\underline{r}_j$  and  $\epsilon_j$  for  $\underline{r}_{0j}$  and  $\epsilon_{0j}$ , respectively. However, different possibilities of reducing computer time have to be examined from case to case.

#### 4. UNDAMPED FREE VIBRATIONS OF A CABLE SUPPORTED ON A SPRING

Free vibrations of cables and strings have been subject to extensive studies [8,28,29,30,31]. We will here discuss free, undamped small amplitude oscillations of a relatively straight (shallow) cable (see (Fig. 4.1)), using basic assumptions presented in [31], where general theories for vibrations of a shallow cable and their application to a "parabolic" cable with fixed support points can be found.

In Section 5.1 a comparison is presented between eigenperiods calculated according to the analytical model given in this section and those calculated by means of the finite element method (FEM). The latter method will, however, not be discussed in this report. It is more general and requires fewer assumptions. The agreement between the two methods is nevertheless good.

Consider Eq. (2.10) and replace  $\underline{f}_r$  with  $\underline{f}^{(1)}$  (buoyancy forces and gravity forces)  $\gamma_0 \ddot{\underline{u}} - \frac{\partial}{\partial s_0} (K(\tilde{\epsilon}_0 + \Delta \tilde{\epsilon})(\underline{x}'_0 + \underline{u}')) - \underline{f}^{(1)} = 0$  (4.1)

The equilibrium configuration is chosen as the reference configuration  $\underline{x}_0$ . Thus, the equilibrium equations associated with Eq. (4.1) are

$$\frac{\partial}{\partial s_0} (K \tilde{\epsilon}_0 \underline{x}'_0) + \underline{f}^{(1)} = 0 \quad (4.2)$$

For small strains  $\tilde{\epsilon}_0$  we may exchange Eq. (4.2) for the equation

$$\frac{\partial}{\partial s_0} (K \frac{\epsilon_0}{1+\epsilon_0} \underline{x}'_0) + \underline{f}^{(1)} = 0 \quad (4.3)$$

For small values of  $\epsilon_0$  it follows from Eq. (2.7) that  $\epsilon_0 \approx \tilde{\epsilon}_0$ , and therefore the solutions of Eqs. (4.2) and (4.3) are anticipated to be similar in character. The solution of Eq. (4.3) is well known [32] and less complicated to handle than Eq. (4.2), and therefore it is used in this study.

At equilibrium the cable hangs in the vertical plane defined by the coordinate axes  $x_1$  and  $x_2$  respectively (Fig. 4.1). Origo is placed at the lowest point of the cable, where also  $s_0 = 0$ . The components of  $\underline{x}_0$  are then obtained from Eq. (4.3),

$$\begin{aligned} x_{01} &= a \operatorname{arcsinh} \left( \frac{s_0}{a} \right) + \frac{\gamma_r g a}{K} s_0 \\ x_{02} &= \sqrt{a^2 + s_0^2} + \frac{\gamma_r g s_0^2}{2K} - a \\ x_{03} &= 0 \end{aligned} \quad (4.4)$$

where  $a$  is a constant. The horizontal component  $H$  of the cable tension is

$$H = \gamma_r g a \quad (4.5)$$

The strain is given by

$$\epsilon_0 = \frac{\gamma_r g}{K} \sqrt{a^2 + s_0^2} \approx \tilde{\epsilon}_0 ; \quad \epsilon_0 \ll 1 \quad (4.6)$$

We will now use the frequently used assumption that the components of  $\underline{u}'$  are small. This assumption is satisfied if also the time dependent strains and

rotations are small and it defines the designation "small oscillations". Combining Eqs.(4.1) and (4.2) we then obtain, neglecting higher order terms,

$$\gamma_0 \ddot{u} - K \frac{\partial}{\partial s_0} (\tilde{\epsilon}_0 \underline{u} + \underline{x}_0 \cdot \underline{u} \underline{x}_0) = 0 \quad (4.7)$$

where  $\underline{x}_0$  and  $\tilde{\epsilon}_0$  are assumed to be defined by Eqs. (4.4) and (4.6), respectively. The tangent vector  $\underline{x}_0$  is obtained by differentiation of Eq. (4.4)

$$\begin{aligned} x_{01}' &= \frac{a}{\sqrt{a^2 + s_0^2}} + \frac{\gamma_r g a}{K} \\ x_{02}' &= \frac{s_0}{a} x_{01}' \end{aligned} \quad (4.8)$$

$$x_{03}' = 0$$

In order to obtain wellknown functions, we exchange the variable  $s_0$  for the new non-dimensional variable  $x$ ,

$$x = \frac{a}{l} \operatorname{arcsinh} \frac{s_0}{a} \quad (4.9)$$

The cable is presumed to oscillate within the interval  $s_0 \in [0, l]$  and it is considered as shallow for small values of  $\theta = l/a$ . Hence, it follows from Eq. (4.9) that  $x \in [0, 1]$ , where  $l \approx 1$ . We also introduce

$$\underline{w} = \frac{\underline{u}}{l} \quad (4.10)$$

Eqs. (4.6) to (4.10) then give

$$\bar{\gamma} \cosh \theta x \begin{bmatrix} \ddot{w}_1 \\ \ddot{w}_2 \end{bmatrix} - \frac{\partial}{\partial x} \left( \alpha \begin{bmatrix} \frac{\partial w_1}{\partial x} \\ \frac{\partial w_2}{\partial x} \end{bmatrix} + \lambda \begin{bmatrix} 1 & , \sinh \theta x \\ \sinh \theta x, \sinh^2 \theta x \end{bmatrix} \begin{bmatrix} \frac{\partial w_1}{\partial x} \\ \frac{\partial w_2}{\partial x} \end{bmatrix} \right) = 0 \quad (4.11a, b)$$

$$\bar{\gamma} \cosh(\theta x) \ddot{w}_3 - \alpha \frac{\partial^2 w_3}{\partial x^2} = 0 \quad (4.12)$$

where

$$\begin{aligned} \lambda &= \frac{1}{\cosh \theta x} \left( \frac{1}{\cosh \theta x} + \alpha \right)^2 \\ \theta &= \frac{l}{a} \\ \bar{\gamma} &= \frac{\gamma_0 l^2}{K} \\ \alpha &= \frac{\gamma_r g a}{K} \end{aligned} \quad (4.13a, b, c, d)$$

Eq. (4.12) is uncoupled with Eq. (4.11), which illustrates the well-known fact that the interaction between the motions in the plane of the cable and those normal to this plane are negligible in this case. Separation of variables in Eq.(4.12) leads to a modified Mathieu equation. The properties of Mathieu equations are described in [33].

The boundary conditions used in this example are

$$\begin{aligned} w_1(l^*, t) &= w_2(l^*, t) = w_3(l^*, t) = 0 \\ w_1(0, t) &= w_3(0, t) = 0 \end{aligned} \quad (4.14a, b, c)$$

$$\frac{\partial w_2}{\partial x}(0, t) = \beta w_2(0, t)$$

where  $\beta = K_f l / \gamma_r g a$  and  $K_f$  is the spring constant of the cable support, see (Fig. 4.1). The time-dependent contribution to the tension is neglected in Eq. (4.14c).

We now assume a shallow cable, i.e. small  $\theta$ -values. Hence,  $\cosh \theta x \approx 1$  and Eq. (4.12) may be simplified to

$$\ddot{\tilde{w}}_3 - \alpha \frac{\partial^2 w_3}{\partial x^2} = 0 \quad (4.15)$$

Assume a solution of the form

$$w_3 = \tilde{w}_3(x) e^{i\omega t} \quad (4.16)$$

where  $\omega$  is the angular frequency. By Eq. (4.15) and the boundary conditions, Eq. (4.14), we obtain: the eigen modes of oscillations normal to the plane of the cable

$$\tilde{w}_{3n}(x) \sim \sin n\pi x \quad n = 1, 2, 3, \dots \quad (4.17)$$

with the eigenperiods

$$T_n = \frac{2l}{n\sqrt{\gamma_r g a}} \quad n = 1, 2, 3, \dots \quad (4.18)$$

The solution of Eq.(4.11) is based on the assumptions proposed in [31]. The cable is assumed to be shallow. We therefore neglect  $\ddot{w}_1$  [31]. This seems to be justified in order to get the first transverse modes. Integration of Eq.(4.11a) then gives

$$\alpha \frac{\partial w_1}{\partial x} + \lambda \left( \frac{\partial w_1}{\partial x} + \frac{\partial w_2}{\partial x} \sinh \theta x \right) = h(t) \quad (4.19)$$

where  $h(t)$  is a time-dependent function and a measure of the contribution to the horizontal component of the cable tension. The coefficient  $\alpha$ , representing the strain in the lowest point of the cable at equilibrium, is much smaller than  $\lambda$ , which is of the order of magnitude of one.

The first term in Eq.(4.19) may thus be neglected, which is consistent with the assumptions made in [31]. Integrating Eq.(4.19) for  $x \in [0, l^*]$  and again using Eq.(4.19) and Eq.(4.11b) we obtain after some algebra

$$\ddot{\tilde{w}}_2 \cosh \theta x - \alpha \frac{\partial^2 w_2}{\partial x^2} + x^{-1} \theta^2 \cosh \theta x \int_0^{l^*} w_2 \cosh \theta x \, dx = x^{-1} \theta \cosh \theta x [w_1 + w_2 \sinh \theta x]_0^{l^*} \quad (4.20a)$$

where

$$x = \int_0^{l^*} \lambda^{-1} dx \quad (4.20b)$$

For a direct solution of Eq.(4.20), reference [33] is of interest. The perturbation method may also be applied (see [34]).

Eq.(4.20) is derived by neglecting the acceleration  $\ddot{w}_1$ , and it is thus valid only for small values of  $\theta$ . We restrict the analysis to first order terms, i.e.  $\cosh\theta x \approx 1$ . Using the boundary conditions Eq. (4.14), we obtain

$$\ddot{w}_2 - \alpha \frac{\partial^2 w_2}{\partial x^2} + x^{-1} \theta^2 \int_0^{l^*} w_2 dx = 0 \quad (4.21)$$

After separation of space- and time-dependent variables, an equation of similar type as the one presented for a parabolic cable in [31] is obtained.

By the separation of variables, using the boundary condition Eq.(4.14a,c) and assuming a harmonic solution, we find the eigenmodes of oscillations in the plane of the cable:

$$\tilde{w}_{2n} \sim \frac{(1 - \csc c_n)}{\csc c_n + \frac{c_n}{\beta}} \csc c_n x + \csc c_n x - \frac{\csc c_n + \frac{c_n}{\beta} \csc c_n}{\csc c_n + \frac{c_n}{\beta}} n \quad (4.22)$$

$n = 1, 2, 3, \dots$

where  $c_n$  is obtained from the transcendental equation

$$c_n (\eta c_n^2 - 1 + \frac{1}{\beta}) \csc c_n + \frac{c_n^2}{\beta} (\eta c_n^2 - 1) \csc c_n + 2(1 - \csc c_n) = 0 \quad (4.23)$$

$n = 1, 2, 3, \dots$

where

$$\eta = \frac{x\alpha}{\theta^2} \quad (4.24)$$

The eigenperiods are

$$T_n = \frac{2\pi l}{c_n} \sqrt{\frac{\gamma_o}{\gamma_r g a}} ; \quad n = 1, 2, 3, \dots \quad (4.25)$$

$l^*$  has been approximated to be 1.0 in Eqs.(4.22) and (4.23).  $x$  in Eq.(4.24) can be calculated using Eqs.(4.13a) and (4.20b) with  $l^* = 1$ . The unstretched length of the cable is  $s_o \approx x l$ .

Eqs.(4.22) and (4.23) may be solved for different values of the parameters  $\eta$  and  $\beta$ , where  $\eta$  expresses the stiffness and the geometry of the cable and  $\beta$  describes the effect of the spring support. It should be noted that Eqs.(4.22) and (4.25) are valid for the first eigenmodes only.

## 5. CALCULATION EXAMPLES

Three calculation examples have been selected to demonstrate the potential of the presented simulation model. The first example deals with a displacement-excited mooring cable (chain). The starting point of the calculation is an equilibrium position generated by constant wind and drift forces acting on the moored structure. Because of the influence of the waves, the structure oscillates around the reference position. A simplified regular oscillating displacement at the upper end has been chosen. The vertical displacement has been disregarded in this example. In the second example comparison is made with an analytical solution in case of displacement excitations out of the plane of the cable.

The third example constitutes a comparison with calculation results presented by Johansson [18].

### 5.1 Displacement-excited mooring cable

Consider a mooring cable (chain) with an equilibrium configuration according to Fig.5.1. The cable hangs in the vertical plane defined by the coordinate axes  $x_1$  and  $x_2$ , respectively. The following data are assumed:

total unstretched length, $L$	= 1200 m
link diameter, $d_o$	= 0.076 m
stiffness, $K$	= $5 \cdot 10^8$ N
density, $\rho_k$	= 7800 kg/m <sup>3</sup>
mass per unit of unstretched length, $\gamma_o$	= 135.35 kg/m
water depth, $D$	= 120 m
density of water, $\rho_v$	= 1000 kg/m <sup>3</sup>
bottom friction coefficient, $\mu$	= 1.0
tolerance according to Fig.3.2, $c_v$	= 0.2 m/s

In order to get some qualitative ideas about the behavior of the cable, we will use the analytical model presented in Section 4 to calculate the eigenperiods of a corresponding undamped system. The part of the cable, which is laying on the bottom, is assumed to be replaceable by a spring support at the touchdown point, (Fig. 4.1 ). This is, of course, a gross simplification of the problem.

The unstretched length from the touchdown point to the upper end of the cable is  $l=507.8$  m. The constant  $a$  given by the elastic catenary, Eq.(4.4), is equal to  $a = 1016.9$  m, then  $\theta = l/a = 0.5$ . The strain at the lowest point of the cable is calculated by Eq.(4.13d),  $\alpha = 0.00235$ , and also  $\eta$  by Eq.(4.24).

Eigenperiods calculated for different conditions by the analytical model and by the finite element model are compared in Tables 5.1 and 5.2.

Table 5.1 Eigenperiods in seconds for oscillations in the plane of the cable

Mode	Analytical model <sup>a)</sup>		Finite element model
	Fixed support,	Weak elastic	Fixed support
	$\beta = \infty$	spring, $\beta = 0$	$\beta = \infty$
1	5.5	7.7	5.8
2	4.2	4.5	4.5
3	3.2	3.6	3.4

a) Eqs. (4.23) and (4.25)

Table 5.2 Eigenperiods in seconds for oscillations out of the plane of the cable

Mode	Analytical model <sup>a)</sup>	Finite element model
1	10.9	11.4
2	5.5	5.7
3	3.6	3.8

a) Eq. (4.18)

The figures presented in the tables should give a fair idea about the magnitude of the resonance periods of a displacement-excited cable with low damping. Possible resonance periods will normally increase due to damping.

The damping effect of the drag forces will be demonstrated later on in this section. The higher period values obtained by means of the finite element method may partly be explained by the inclusion of the hydrodynamic mass in this model. However, drag-damping is excluded.

In the time-dependent simulation the following displacement was assumed at the upper end of the cable.

$$\begin{aligned}
 u_i(L, t) &= A_i \frac{t}{t_k} \sin \frac{2\pi}{T_p} t & t < t_k \\
 u_i(L, t) &= A_i \sin \frac{2\pi}{T_p} t & t \geq t_k
 \end{aligned}
 \tag{5.1}$$

$$i = 1, 3$$

$$u_2(L, t) = 0$$

Calculations have been made for different values of  $A_i$ ,  $T_p$  and  $t_k$  (see Table 5.3). The displacement functions for case 1, 2, and 3 are shown also in Figs. 5.2 and 5.3.



Table 5.3 Combinations of parameter values used in the simulations

Calculation case	ND	NE	$A_1$ (m)	$A_3$ (m)	$C_{DN}$	$C_{DT}$	$C_{MN}$	$t_k$ (s)	$T_p$ (s)	$\Delta t$ (s)	Slack
1	3	40	5.08	2.1	2.5	0.5	3.8	45	15	0.01	Yes
2	3	40	5.08	2.1	1.0	0.2	3.8	45	15	0.01	No
3	3	40	5.08	2.1	0.5	0.1	3.8	45	15	0.01	No
4	3	40	5.08	0.0	2.5	0.5	3.8	45	15	0.01	Yes
5	2	20	5.08	-	2.5	0.5	3.8	45	15	0.01	Yes
6	3	40	5.08	0.0	2.5	0.5	3.8	40	20	0.01	No

ND = 2 : two-dimensional calculation

ND = 3 : three-dimensional calculation

NE : number of elements of equal length (see Fig.5.4)

$\Delta t$  is calculated from Eq.(3.34).

Different values were assumed for  $C_{DN}$  and  $C_{DT}$  (see Table 5.3). The coefficients are related to the link diameter  $d_o$  of the chain. There seems to be a lack of relevant experimental studies with regard to chain profiles.

The calculations 1, 4, and 5 were performed with an excitation period  $T_p = 15s$  and with high values of the drag force coefficients. In all three cases, slack (negative strain,  $\epsilon < 0$ ) was obtained after 53s, see Table 5.4. The calculations were then terminated.

Table 5.4 Summary of slack appearance

Calculation case	ND	NE	Slack appeared		Touchdown point at node number
			in element number	at time (s)	
1	3	40	8	53.6	24
4	3	40	7	53.6	24
5	2	20	8	53.2	13

The tension in the upper end element was practically equal in all three cases (1, 4 and 5). Case 1 is shown in Fig. 5.5. The reason that the force is the same, irrespective of the calculations being two- or three-dimensional may be explained by small strains and rotations. Oscillations out of the plane of the cable then give negligible contributions to the tension (see Section 4).

Fig. 5.5 displays the tension in the upper end element for different values of the drag force coefficients,  $C_{DN}$  and  $C_{DT}$ . In case 3, where the lowest values of the coefficients have been used, the force may be regarded as more or less quasi-static, i.e. the force can be estimated from the elastic catenary. This seems reasonable also from a comparison between the excitation period (15s) and the estimated undamped eigenperiods.

Fig. 5.5 also shows that the tension increases with increasing drag force coefficient values. For the highest values used, case 1, slack is obtained. The obvious conclusion from these numerical experiments is that high drag forces may give rise to slack conditions, that is, negative strain. We conclude that the properties of the system have changed radically because of the high drag forces.

Immediately after a slack situation a longitudinal impact has to be anticipated. However, it is not obvious which theoretical model to use under these conditions. In the case of a chain, it might be justified to assume zero tension if the strain is negative. This is a frequently used model which is easy to program. However, we also have to check a basic assumption for the validity of the equations of motion,

$$\underline{x}(s_k, t) \neq \underline{x}(s_l, t) \quad s_l \neq s_k$$

that is, different material points on the cable are not allowed to meet. This criterion may require time-consuming checking procedures. Under certain conditions, it might therefore be justified to use the simpler criterion  $\epsilon > -1$ . However, modeling with regard to slack requires further investigations.

When the excitation period was increased, the tension decreased (case 4 and 6, see Fig. 5.6). No slack situation appeared in case 6 ( $T_p = 20s$ ).

In case 2 the tension is (Fig. 5.5) stationary after about 45s. However, this does not hold for all variables. Figs. (5.7) and (5.8) show the displacement of node 24 (the touchdown point in equilibrium) in the vertical plane (direction 2) and out of the plane of the cable (direction 3), respectively. The nodes thus drift in direction 3.

## 5.2 Comparison with analytical solution

The numerical time dependent solution is compared with an analytical solution based on the theory presented in Section 4. Assume the touchdown point to be kept fixed and the cable (same as in sect. 5.1) to be at equilibrium at time  $t=0$ . The upper end is exposed to a displacement excitation out of the plane of the cable:

$$\begin{aligned} u_3(l, t) &= A_3 \sin \frac{2\pi}{T_p} t \\ u_2(l, t) &= u_1(l, t) = 0 \end{aligned} \tag{5.2}$$

The cable (counted from the touchdown point to the upper end,  $l = 507.8$  m) is divided into 20 elements. If only lift forces and gravity forces are considered ( $C_{DT} = C_{DN} = C_{MN} = 0$ ), an approximate solution may be obtained from Eq. (4.15) assuming that the oscillations are "sufficiently small". This solution is here obtained as a Fourier series with 80 components. Figs. (5.9) and (5.10) display analytically and numerically calculated displacements at the midpoint of the cable ( $s_0 = 1/2$ ) for two different amplitudes  $A_3$ . The excit-

ation period  $T_p$  is 15s.

According to the linear theory the tension in the cable is presumed to be constant and equal to the static one, in the case of small vibrations out of plane of the cable. The numerical solutions resulted in the following relative tensions in the upper end element

$$\begin{array}{ll} A_3 = 2.5 \text{ m} & T_{\text{numerical}}^{\text{max}}/T_{\text{static}} = 1.023 \\ A_3 = 10.0 \text{ m} & T_{\text{numerical}}^{\text{max}}/T_{\text{static}} = 1.40 \end{array}$$

Thus, large excitation amplitudes result in an increased cable tension.

When the excitation period was changed from 15s to 12s, the increase in cable tension became considerable and slack appeared. The 12s period is close to the eigenperiod value of 10.9s estimated by means of linear theory.

The agreement between displacements obtained by the analytical solution and the numerical solution (Fig.5.9, 5.10) is satisfactory, in spite of the disagreement in tension. The small discrepancies may be referred to "errors" in both the analytical solution (too large  $\theta = 1/a$ ) and the numerical solution (for example discretization error).

A completely stretched cable and a hanging cable are other examples for which analytical solutions can be used for comparison. However, we do not know of any analytic solutions also considering geometrical non-linearities and non-linear drag forces. Mathematical analysis are in progress for certain cases [35].

### 5.3 Comparison with tests presented by Johansson [18].

Johansson [18] presented some calculation tests, one of which has been selected for a comparative test.

The simulation model constructed by Johansson also makes use of a displacement-based finite element method with linear shape functions. (In our model, an exception is made with regard to linear shape functions in Eq.(3.8) in order to obtain an easily invertible mass matrix). The time integration method is, on the other hand, quite different (for a comparison see [18]).

Data and results presented by Johansson have been transformed into the units and constants used in our study. Even if the transformation is not entirely exact, it is accurate enough to make a comparison meaningful.

Consider a cable hanging in water at equilibrium at time  $t = 0$  (see Fig.5.11). The following cable data are assumed:

mass per unit of unstretched length, $\gamma_O$	= 24.7 kg/m
stiffness, $K$	= $2.28 \cdot 10^8$ N
unstretched length (calculated by us), $L$	= 1040.94 m
drag force coefficient, $C_{DN}$	= 1.4
	, $C_{DT}$ = 0.0
mass coefficient, $C_{MN}$	= 1.2
density, $\rho_k$	= 5440 kg/m <sup>3</sup>
diameter, $d_O$	= 0.076 m

The density of water is  $\rho_v = 1000 \text{ kg/m}^3$ . The cable is divided into 10 equal elements according to [18]. The static tension in the upper element was calculated by the finite element method to be  $5.6 \cdot 10^5 \text{ N}$ .

The calculation example is a two-dimensional problem. The upper end of the cable is given the following displacement:

$$\begin{aligned}
 u_1(L, t) &= 1.414 \frac{t}{2} & t < 2s \\
 u_2(L, t) &= 2.5 \frac{t}{2} & t < 2s \\
 u_1(L, t) &= 1.414 & t \geq 2s \\
 u_2(L, t) &= 2.5 & t \geq 2s
 \end{aligned} \tag{5.3}$$

The upper end is pulled a certain distance at constant velocity for 2 seconds and then held fixed in the extreme position.

The time step in our calculation is  $\Delta t = 0.02 \text{ s}$ . Johansson used 0.25s except for the initial phase when time steps down to 0.01s were used.

Fig.5.12 shows the calculated tension in element 6, counted from the lower end of the cable. (Johansson [18] presented the dynamic part of the tension which has been added by us to the static tension). Johansson's solution is smoother than ours since he introduced a proportional viscous damping simulating the internal friction of the cable. The damping constant was given the value  $c_c = 2.3 \cdot 10^8 \text{ Ns/m}^2$ . However he reports in [18] that after the calculations had been done, values were found [36] for steel wire ropes of the order of magnitude of  $c_c \approx 1.5 \cdot 10^7 \text{ Ns/m}^2$ .

Our curve is plotted on the basis of the value calculated at every tenth time step (the interval is 0.2s). As our calculation does not consider any tangential drag damping ( $C_{DT} = 0$ ) or any internal damping, longitudinal oscillations are obtained.

If our curve is smoothed, a good agreement is obtained with Johansson's solution. The vertical displacement calculated at the node 6, however, does not exhibit any significant oscillations (Fig. 5.13).

## 6. SUMMARY AND CONCLUSIONS

A numerical simulation model for the calculation of the dynamic response of mooring cables has been developed. The finite element method is used for the discretization of the cable into a number of elements, leading to a system of equations of motion of a discrete system. These equations are solved in the time domain by means of a simple explicit difference scheme.

The model takes into account non-linearities caused by a change of the geometry of the cable, drag forces, and contact and friction between the cable and the sea bottom.

A comparative calculation test showed good agreement with results obtained by Johansson [18]. Reasonable agreement was obtained also with analytical solutions. However, more systematic analysis must be undertaken in order to test the convergence of the numerical model with respect to errors due to the spatial discretization and the time integration method.

An analysis of the properties of a displacement-excited mooring cable (chain) is presented. The first eigenperiods of the undamped system were estimated by a simplified model to be lower than the period of the displacement excitation. In the case of low damping (*i.e.* small values of the drag force coefficients) an almost quasi static solution was obtained, which seems reasonable considering the relative magnitude of the periods. At high damping, slack (*i.e.* negative strain) was obtained in the cable at about the same point of time for different numbers of elements, regardless of whether two- or three-dimensional calculations were performed. The example shows that the drag forces can have significant effects on the dynamic response of mooring cables.

Also the calculated cable tension had about the same value in the two-dimensional as in the three-dimensional calculation, which may be explained by the small displacements in this example. General conclusions concerning the necessity of three dimensional calculations are, however, always difficult to draw due to the nonlinear character of the problem. Three-dimensional calculation was found to require a rather long time of integration for "steady-state" to be obtained.

Further development of the model is planned with respect to the formulation of the slack condition. In addition, the model will be modified to make possible an analysis of the effect of geometrical non-linearities. Some experimental studies are also planned.

### ACKNOWLEDGEMENTS

The authors wish to express their gratitude to Dr. Christian Högfors, Department of Mechanics, Chalmers University of Technology, for many valuable discussions and advice during the course of this study. We also wish to thank Dr. Lars Bergdahl and our colleagues within the project "Offshore Structures, Wave Forces and Motions" for their participation in and support of the work.

## REFERENCES

- [1] Løken, A.E. and Olsen, O.A.: "The Influence of Slowly Varying Wave Forces on Mooring Systems". OTC. Texas (April 30 - May 3, 1979).
- [2] Jain, R.K.: "A Simple Method of Calculating the Equivalent Stiffness in Mooring Cables". Applied Ocean Research, (1980), Vol. 2, No. 3.
- [3] Wilson, B.W. and Garbaccio, D.H.: "Dynamics of Ship Anchor-Lines in Waves and Current". Journal of the Waterways and Harbours Division (Nov. 1969).
- [4] Furuholt, E.: "Mooring Systems for Offshore Operations". Norwegian Maritime Research No. 4 (1975).
- [5] Ali, S. and Shore, S.: "Forced Nonlinear Vibration of Sagged Cables". Int. Conf. in Computer Methods in Nonlinear Mechanics, Austin, Texas, (1974).
- [6] Watts, A.M. and Frith, R.H.: "Efficient Numerical Solution of Dynamic Equations of Cables". Computer Methods in Applied Mechanics and Engineering 25 (1981) pp.1-9.
- [7] Maltuk, C.: Impact Damping and Airplane Towing. Doctoral Thesis. Division of Solid Mechanics, University of Luleå, Sweden (1982).
- [8] Nayefeh, A.H. and Mook, D.T. Nonlinear Oscillations, John Wiley & Sons, New York (1979).
- [9] Nath, J.H. and Felix, M.P.: "Dynamics of Single Point Mooring in Deep Water". Journal of Waterways, Harbors and Coastal Engineering Division. (November, 1970).
- [10] Huffmann, R.R. and Genin, J.: "The Dynamical Behaviour of a Flexible Cable in a Uniform Flow Field". The Aeronautical Quarterly (May 1971).
- [11] Walton, T. and Polacheck, H.: "Calculation of Nonlinear Transient Motion of Cables". Department of the Navy. DAVID TAYLOR MODEL BASIN. Report 1279 (July 1959).
- [12] Winget, J.M. and Huston, R.L.: "Cable Dynamics - A Finite Segment Approach". Computer & Structures, Vol. 6, pp. 475-480 (1976).
- [13] Huston, R.L. and Kamman, J.W.: "A Representation of Fluid Forces in Finite Segment Cable Models". Computers & Structures, Vol. 14, No. 3-4, pp. 281-287, (1981).
- [14] Dominques, R.F. and Smith, C.E.: "Dynamic Analysis of Cable Systems". Journal of the Structural Division. Proc. of the ASCE, Vol. 98, ST8 (Aug. 1972).
- [15] Leonard, J.W. and Recker, W.W.: "Nonlinear Dynamics of Cables with Low Initial Tension". Journal of the Engineering Mechanics Division (April 1972).
- [16] Leonard, J.W.: "Incremental Response of 3-D Cable Networks". Journal of the Engineering Mechanics Division (June 1973).
- [17] Leonard, J.W.: "Nonlinear Dynamics of Curved Cable Elements". Journal of the Engineering Mechanics Division. (June 1973).
- [18] Johansson, P.I.: A Finite Element Model for Dynamic Analysis of Mooring Cables. Massachusetts Institute of Technology, Ph.D. Thesis (Jan. 1976).
- [19] Webster, R.L.: An Application of the Finite Element Method to Determination of Nonlinear Static and Dynamic Responses of Underwater Cable Structures. Cornell University, Ph.D. Thesis (January 1976).

- [20] Sander, G., Geradin, M., Nyssen, C. and Hogge, M.: "Accuracy Versus Computational Efficiency in Nonlinear Dynamics". Computer Methods in Applied Mechanics and Engineering 17/18 (1979) 315-430.
- [21] Goodman, T.R. and Breslin, J.P.: "Statics and Dynamics of Anchoring Cables in Waves". Journal of Hydronautics (October 1976).
- [22] Triantafyllou, M.S.: "Preliminary Design of Mooring Systems". Journal of Ship Research, Vol. 26, No. 1 (March 1982) pp. 25-35.
- [23] Routh, E.J.: Dynamics of Systems of Rigid Bodies, 6th ed. New York (1955).
- [24] Szabo, I.: Höhere Technische Mechanik 2.Aufl. Berlin-Göttingen-Heidelberg (1958).
- [25] Casarella, M.J. and Parsons, M.: "Cable Systems Under Hydrodynamic Loading". Marine Technology Society Journal Vol. 4, No. 4 (July-August 1970).
- [26] Bathe, K.J. and Wilson, E.L.: Numerical Methods in Finite Element Analysis. Prentice-Hall, Inc., Englewood Cliffs, New Jersey (1976).
- [27] Engelman, M.S., Strang, G. and Bathe, K.J.: "The Application of Quasi-Newton Methods in Fluid Mechanics". International Journal for Numerical Methods in Engineering, Vol. 17, 707-718 (1981).
- [28] Saxon, D.S. and Cahn, A.S.: "Modes of Vibration of a Suspended Cable", Quarterly Journal of Mechanics and Applied Mathematics, Vol. VI, Part 3, (1953), pp. 273-285.
- [29] Irvin, M.H.: "Studies in the Statics and Dynamics of Simple Cable Systems. Thesis. California Institute of Technology, Pasadena California (1974).
- [30] Pugsley, A.G.: "On the Natural Frequencies of Suspension Chains". Quarterly Journal of Mechanics and Applied Mathematics, Vol. II, Part 4, (1949), pp. 412-418.
- [31] Møllmann, H.: A Study in the Theory of Suspension Structures. AKADEMISK FORLAG, Denmark (1965).
- [32] Ramsey, A.S.: Statics . Cambridge, The University Press. (1960).
- [33] McLachlan, N.W.: Theory and Application of Mathieu Functions. University Press Oxford (1951).
- [34] Nayfeh, A.H.: Perturbation Methods . John Wiley & Sons, New York (1973).
- [35] Ames, W.F., Lohner, R.J. and Adams, E.: "Group Properties of  $u_{tt} = [f(u)u_x]_x$ ". Int.J.Non-Linear Mechanics. Vol. 16, No. 5/6, pp.439-447, (1981).
- [36] Kawashima, S. and Kimura, H.: "Measurement of the Internal Friction of Metal Wires and Metal Wire Ropes through the Longitudinal Vibration". Mem. Fac. Engr. Kyushu University, 13 (1), (1952).

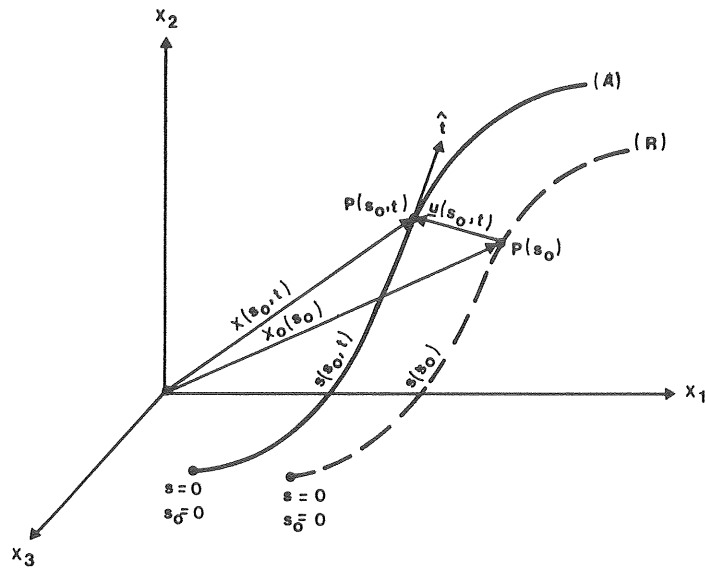


Fig. 2.1 Reference configuration (R) and actual configuration (A) in a rectangular Cartesian coordinate system.

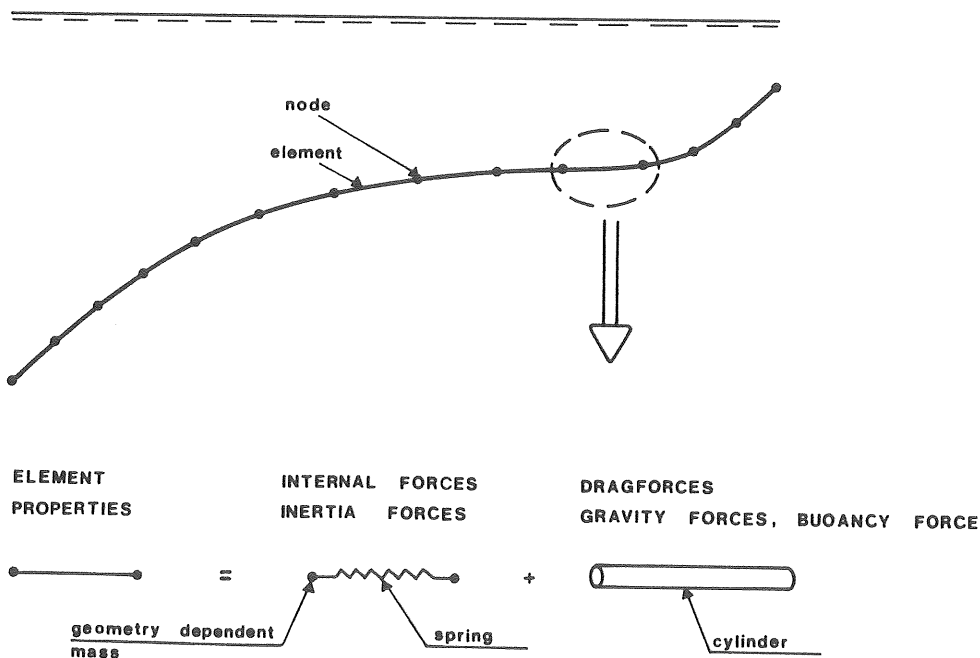


Fig. 3.1 Discretized system.



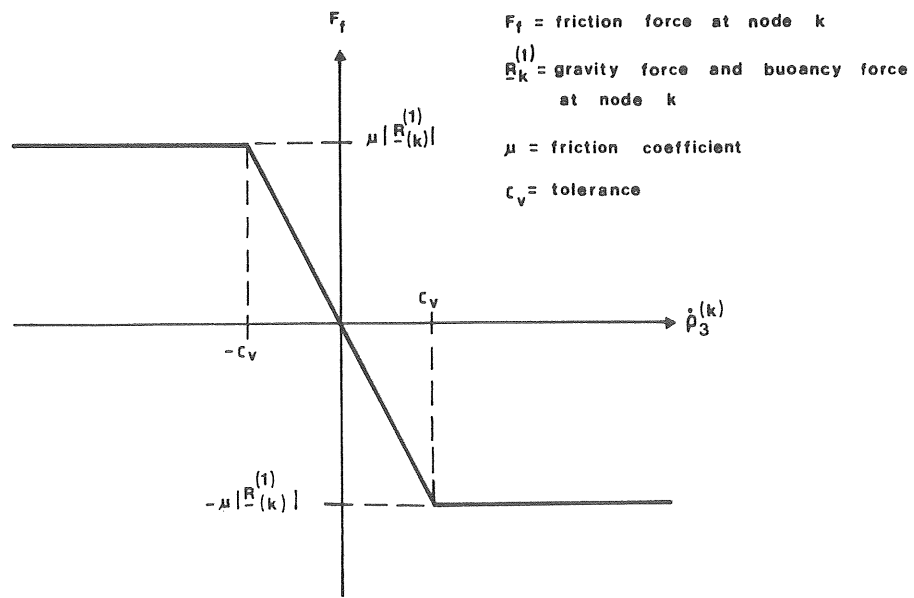


Fig. 3.2 Formulation of the frictional force  $F_f$ .

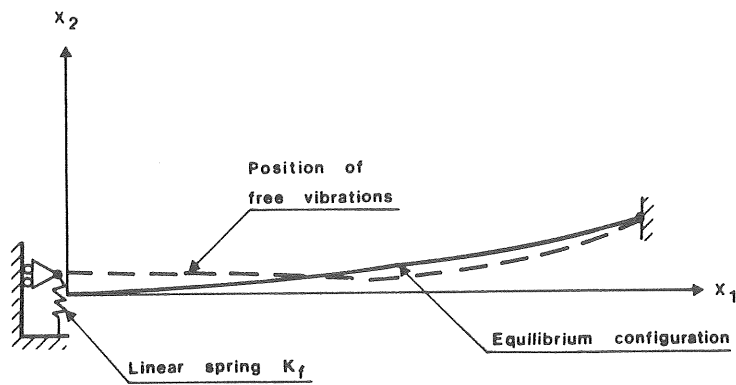


Fig. 4.1 Simplified cable model.

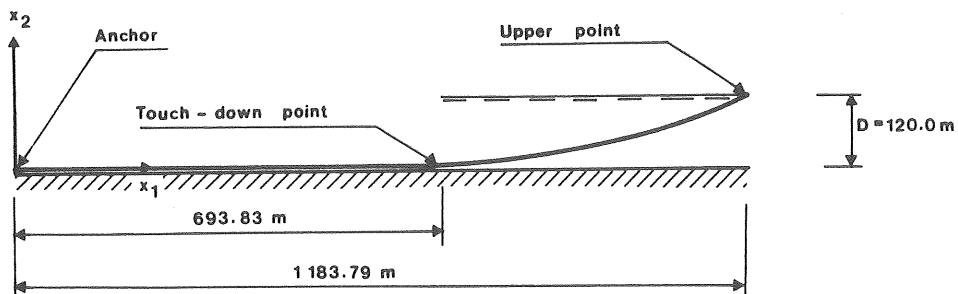


Fig. 5.1 Equilibrium configuration of the cable.

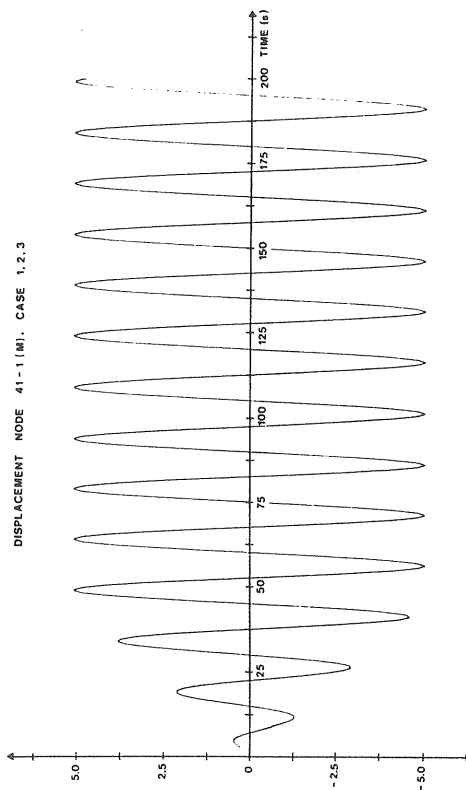


FIG. 5.2 PRESCRIBED DISPLACEMENT AT THE UPPER END

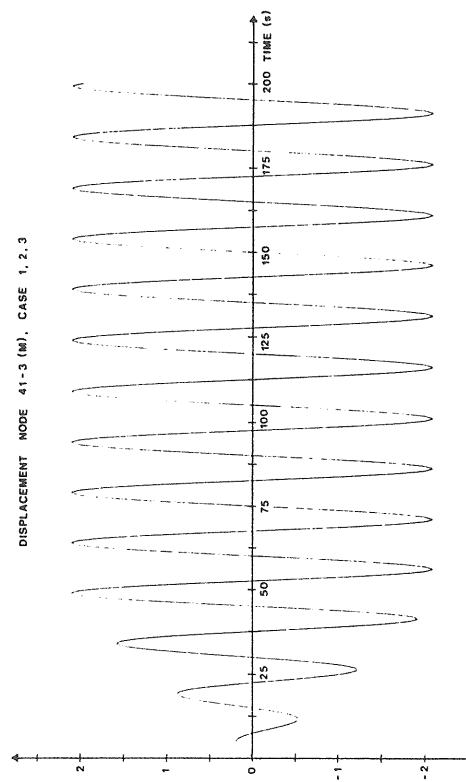
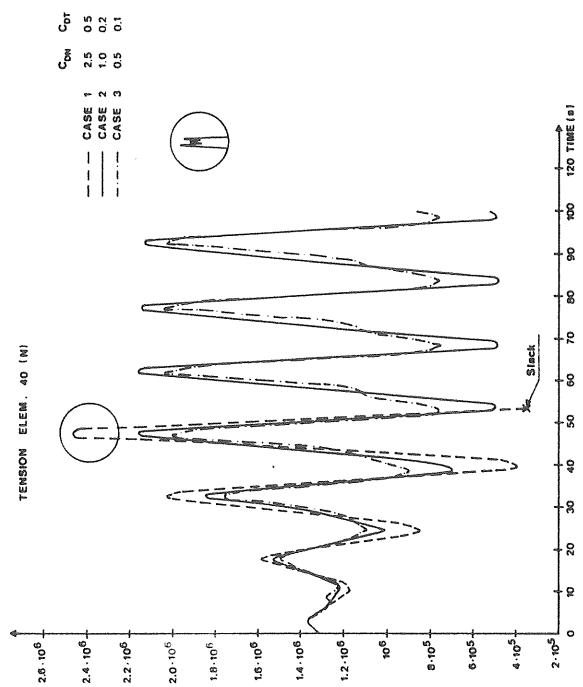
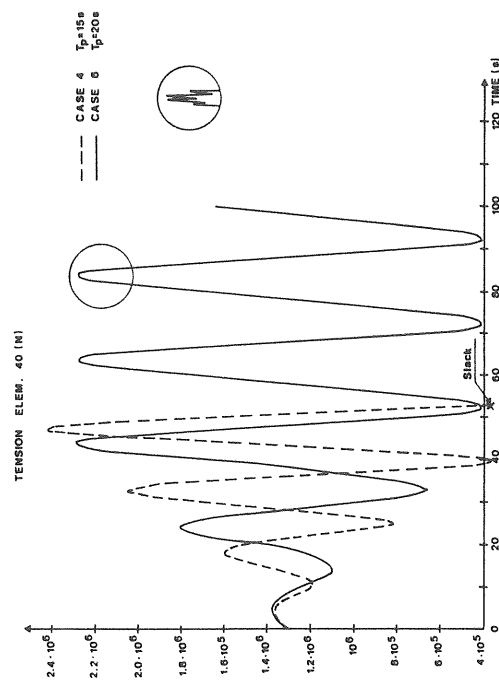
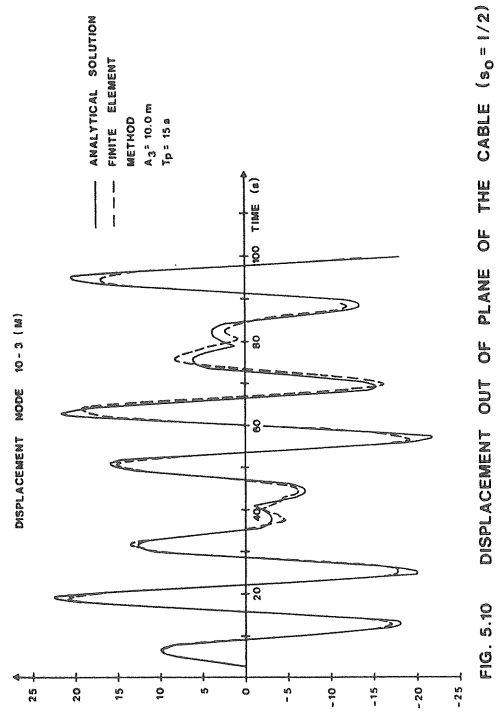
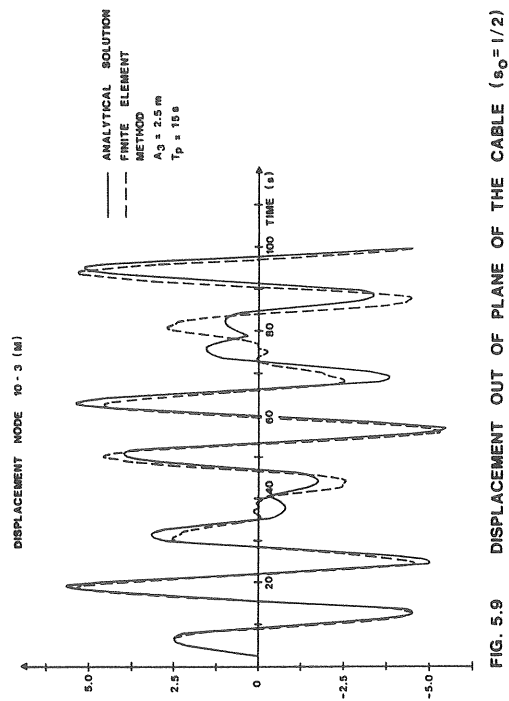
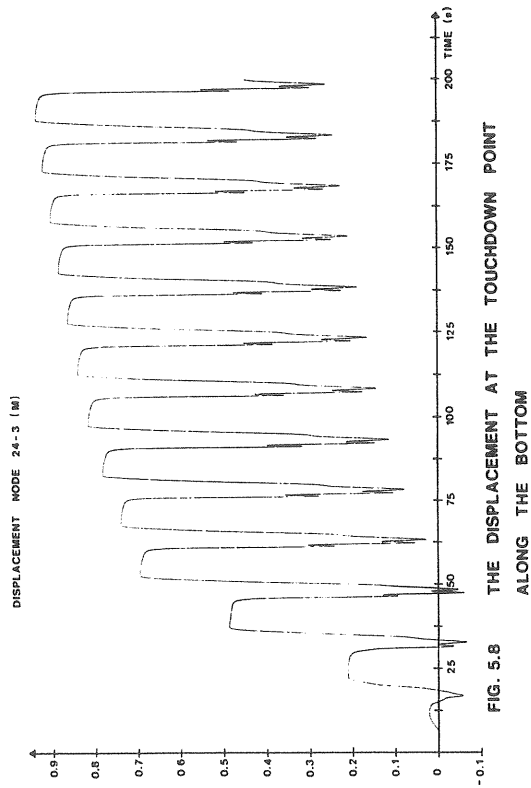
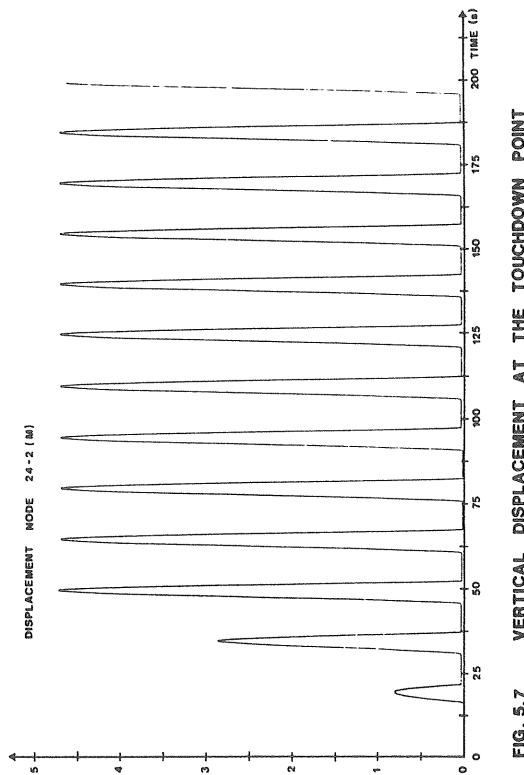


FIG. 5.3 PRESCRIBED DISPLACEMENT AT THE UPPER END

FIG. 5.5 TENSION IN ELEMENT 40 FOR DIFFERENT CDT, C<sub>DN</sub>FIG. 5.6 TENSION IN ELEMENT 40 FOR DIFFERENT T<sub>p</sub>



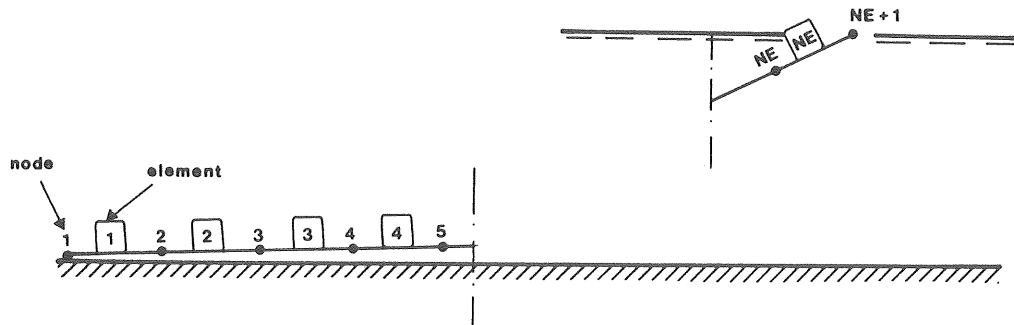


Fig. 5.4 Numbering of nodes and elements.

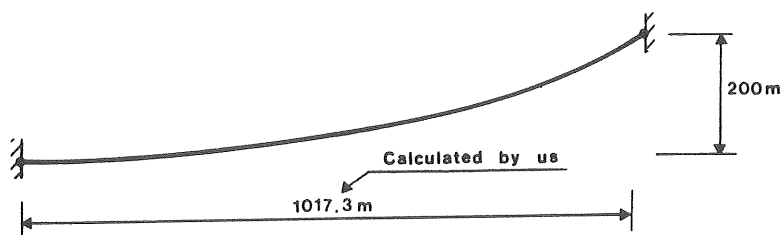


Fig. 5.11 Equilibrium configuration of the cable in the comparative test.

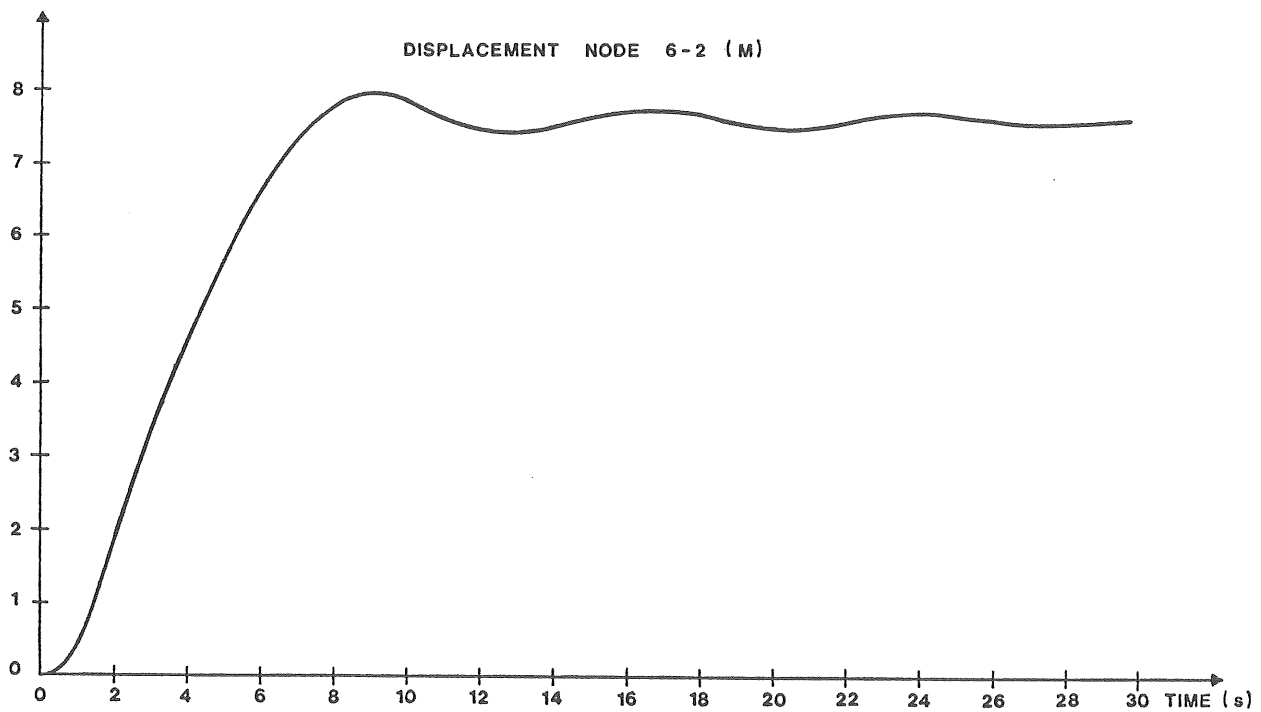


Fig. 5.13 Vertical displacement at node 6 in the comparative test.

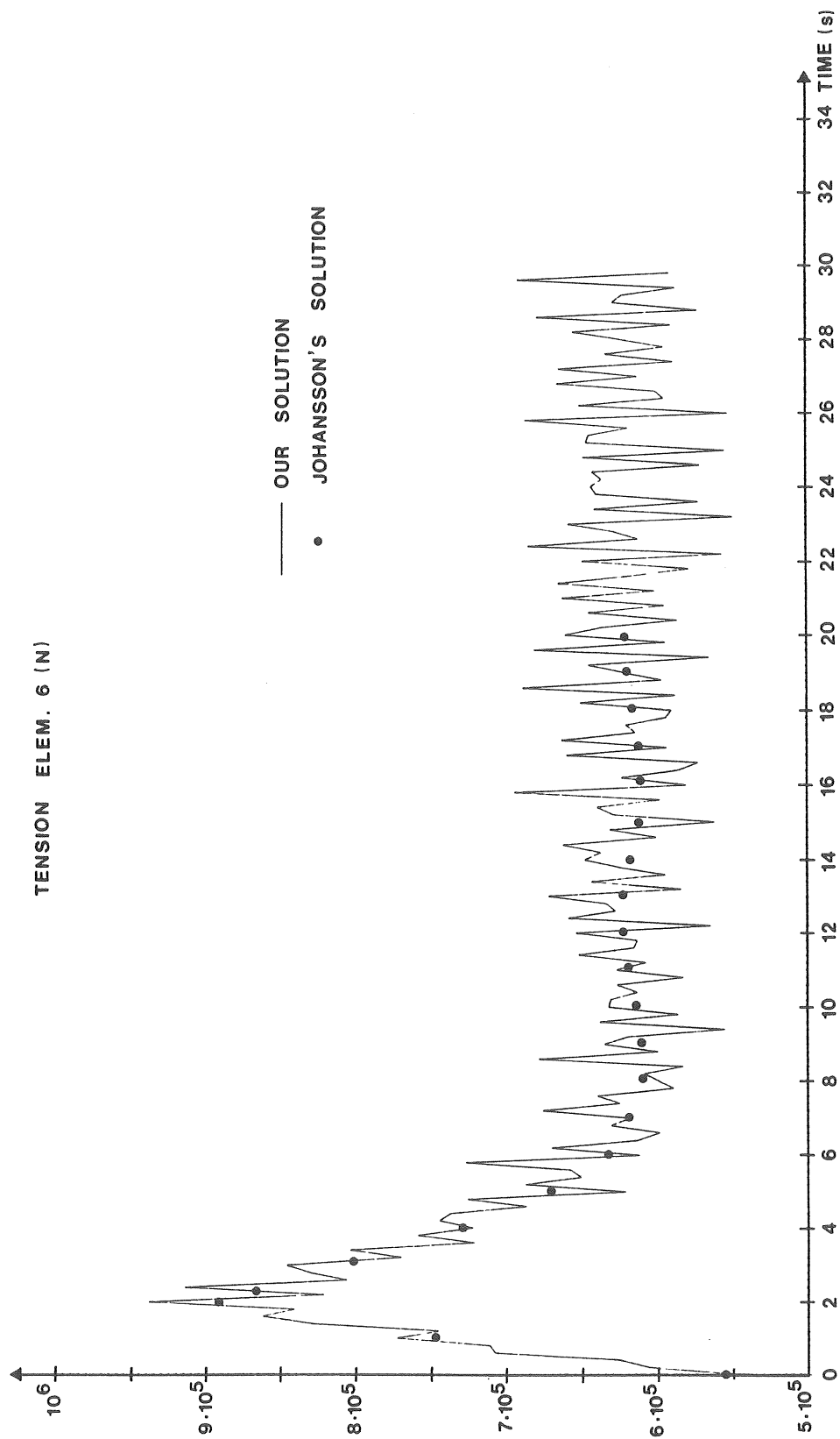


Fig. 5.12 Tension in element 6, in the comparative test.

Department of Hydraulics  
Chalmers University of Technology

Report Series A

- A:1 Bergdahl, L.: Physics of ice and snow as affects thermal pressure. 1977.
- A:2 Bergdahl, L.: Thermal ice pressure in lake ice covers. 1978.
- A:3 Häggström, S.: Surface Discharge of Cooling Water. Effects of Distortion in Model Investigations. 1978.
- A:4 Sellgren, A.: Slurry Transportation of Ores and Industrial Minerals in a Vertical Pipe by Centrifugal Pumps. 1978.
- A:5 Arnell, V.: Description and Validation of the CTH-Urban Runoff Model. 1980.
- A:6 Sjöberg, A.: Calculation of Unsteady Flows in Regulated Rivers and Storm Sewer Systems. (in Swedish). 1976.
- A:7 Svensson, T.: Water Exchange and Mixing in Fjords. Mathematical Models and Field Studies in the Byfjord. 1980.
- A:8 Arnell, V.: Rainfall Data for the Design of Sewer Pipe Systems. 1982.
- A:9 Lindahl, J. och Sjöberg, A.: Dynamic Analysis of Mooring Cables. 1983.

